National Park Service
U.S. Department of the Interior

Golden Gate Bridge (center), City of San Francisco (back), and Golden Gate National Recreation Area (front and right) (photo P. Gonzalez)

Climate Change in the National Parks of the San Francisco Bay Area, California, USA

Patrick Gonzalez, Ph.D.

Natural Resource Stewardship and Science
U.S. National Park Service
130 Mulford Hall
University of California, Berkeley
Berkeley, CA 94720-3114 USA

July 11, 2016

Abstract

Greenhouse gas emissions from human activities have caused global climate change and widespread impacts on physical and ecological systems. To assist in the integration of climate change science into resource management in the nine U.S. national parks in the San Francisco Bay Area, California, including Golden Gate National Recreation Area (NRA), Muir Woods National Monument (NM), Point Reyes National Seashore (NS), and six other parks, this report presents: (1) results of original spatial analyses of historical and projected climate change trends at 800 m spatial resolution, (2) results of a systematic scientific literature review of historical impacts, future vulnerabilities, and ecosystem carbon, focusing on research conducted in the parks, and (3) results of original spatial analyses of ecosystem carbon at 30 m spatial resolution. For the areas within the boundaries of each park, average annual temperature from 1950 to 2010 increased at statistically significant rates of up to 2.4 ± 0.7ºC (4.3 ± 1.3ºF.) per century (mean ± standard error), with the greatest increases in spring. Total annual precipitation from 1950 to 2010 showed no statistically significant change. Published analyses of field research that includes data from the nine parks detected changes that have been attributed to human climate change. These include a 22 cm (8.6 in.) increase of sea level since 1854 and northward shifts of winter bird ranges of 0.5 ± 0.3 km (0.3 ± 0.2 mi.) per year from 1975 to 2004. With continued emissions of greenhouse gases, projections under the four emissions scenarios of the Intergovernmental Panel on Climate Change (IPCC) indicate annual average temperature increases of up to 3.8 ± 0.8ºC (6.8 ± 1.4º F.) (mean ± standard deviation) from 2000 to 2100. Climate models project increases of total annual precipitation of 5% to 10% on average, but increased temperatures may still increase aridity. Published analyses that cover the area of the nine parks identify numerous future vulnerabilities to climate change, including increased drought risk for coast redwoods, changes in distributions of major vegetation types, reduced populations of four rare plant species, reduced coastal habitat for birds and marine mammals due to sea level rise, and flooding of cultural resources and infrastructure by sea level rise and storm surge. National park ecosystems can help to naturally reduce climate change by storing carbon. Aboveground vegetation in the natural ecosystems of the parks stores an amount of carbon equivalent to the annual emissions of 370 000 ± 140 000 Americans (mean ± 95% confidence interval). Coast redwoods (*Sequoia sempervirens*) adjacent to Muir Woods NM contain carbon at densities of 970 ± 50 t ha^{-1}, higher than many other forests around the world. From 2001 to 2010, aboveground carbon in the San Francisco Bay Area parks increased.

Introduction

Greenhouse gas emissions from power plants, motor vehicles, deforestation, and other human activities have increased temperatures around the world and caused other changes in climate in the 20th and early 21st centuries (IPCC 2013). Field measurements show that climate change is fundamentally altering ecosystems by shifting biomes, contributing to species extinctions, and causing numerous other changes (IPCC 2014). To assist in the integration of climate change science into management of natural, cultural, infrastructure, and other resources in the U.S. national parks of the San Francisco Bay Area, California, this report presents results of original spatial analyses of historical and projected climate change and ecosystem carbon and a summary of published scientific findings on historical impacts of climate change and future vulnerabilities.

The nine U.S. national parks in the San Francisco Bay Area, California, (Figure 1) are:

Eugene O'Neill National Historic Site
Fort Point National Historic Site
Golden Gate National Recreation Area
John Muir National Historic Site
Muir Woods National Monument
Point Reyes National Seashore
Port Chicago Naval Magazine National Memorial
Rosie the Riveter WWII Home Front National Historical Park
San Francisco Maritime National Historical Park

Methods

The historical analyses (Wang et al., in preparation) used previously published spatial climate data layers at 800 m spatial resolution, derived from point weather station measurements using the Parameter-elevation Relationships on Independent Slopes Model (PRISM; Daly et al. 2008). This data set uses weather station measurements and interpolates between weather stations based on elevation and topography. The spatial analysis area for an individual park is the area within its boundaries. This report presents spatial results for each of the three parks with the most extensive land area and combines the other six parks into a single group. In addition, climate change results are reported separately for the entire area within the legislative boundary of Golden Gate NRA, the portion of that area managed by Golden Gate NRA, and for the parts

of the management area north and south of the Golden Gate.

Linear regression of temperature and precipitation time series gives the historical climate trends, with the statistical probability of significance corrected for temporal autocorrelation. The period starting in 1950 gives a more robust time series than the period starting in 1895 because the U.S. Government established a substantial number of weather stations in the late 1940s and the weather station network has been relatively stable since then. Spatial data from the longer period relies on fewer weather stations and a network that changed irregularly before the 1940s.

The spatial analyses of future projections (Wang et al., in preparation) use output of all available general circulation models (GCMs) of the atmosphere in the Coupled Model Intercomparison Project Phase 5 (CMIP5) data set established for the most recent IPCC report (IPCC 2013). The coarse GCM output, at spatial resolutions of up to 200 km, has been downscaled to 800 m spatial resolution using bias correction and spatial disaggregation (BCSD; Wood et al. 2004).

The information on historical impacts of climate change and future vulnerabilities comes from a search of the Thomson Reuters Web of Science scientific literature database for published research that used field data from the nine parks or analyses that included the San Francisco Bay Area.

Historical Climate Changes

For each of the nine national parks, mean annual temperature showed statistically significant increases in the periods 1895-2010 and 1950-2010 (Figure 2, Tables 1, 2, 3, 5, 7). The 1950-2010 trends show the greatest rate of warming in spring (Tables 3, 5, 7). For the State of California as a whole, the high rates of heating in the spring are attributable to human global emissions of greenhouse gases (Bonfils et al. 2008). The highest rates of warming have occurred in the North Bay north of Muir Woods NM and in the South Bay around the City of San Jose (Figure 3).

For all nine national parks, total annual precipitation for the periods 1895-2010 and 1950-2010 showed no statistically significant trends, with the precipitation slightly increasing in the shorter time period and slightly decreasing in the longer time period (Figure 4, Tables 1, 2, 4, 6, 8). Total annual precipitation decreased north of the Golden Gate, including most of the area of Muir

Woods NM and Point Reyes NS (Figure 5). The precipitation graph (Figure 4) shows the annual data for 2011-2013, years of a severe California drought. Analysis of 1950-2013 precipitation found no statistically significant trends.

Climate water deficit, the difference between precipitation and actual evapotranspiration, increased across the San Francisco Bay Area, except for much of the City of San Francisco and parts of the East Bay, including the area of Eugene O'Neill NHS, between the periods 1900-1939 and 1970-2009, indicating that conditions became more arid (Rapacciuolo et al. 2014).

Analyses of the difference of coast and inland summer maximum temperatures, which is an indicator of fog, from California, Oregon, and Washington, and fog measurements from Arcata and Monterey, California, indicate that fog decreased one-third between the periods 1901-1925 and 1951-2008 (Johnstone and Dawson 2010).

National Oceanic and Atmospheric Administration (NOAA) analyses of weather station data show an increase in the southwestern U.S. of heavy storms, with the decade 1991-2000 experiencing an increase of 25% in five-year storms (a storm with more precipitation than any other storm in five years), compared to the 1901-1960 average (Walsh et al. 2014). NOAA analyses show a 5% increase in the amount of precipitation falling in the heaviest 1% of all daily storm events from 1958 to 2012 in the southwestern U.S. (Walsh et al. 2014).

A severe drought struck most of California, including the parks of the San Francisco Bay Area, from 2012 to 2014, with the lowest 12-month precipitation total combining with the hottest annual average temperature (Diffenbaugh et al. 2015). Analyses of the Palmer Drought Severity Index (PDSI), an indicator of near-surface soil moisture, for the period 1901-2014 indicate that 2014 was the driest year in the record for Golden Gate NRA south of the Golden Gate and was one of the ten driest years for most of the region's other national parks (Williams et al. 2015). Analyses of PDSI for the period 1896-2014 showed that, while the probability of low precipitation years has not increased, the hotter temperatures caused by human climate change have increased the probabilities of drought through increased probabilities of high temperature and low precipitation co-occurring in a single year (Diffenbaugh et al. 2015). For the State of California as a whole, human climate change accounted for one-tenth to one-fifth of the 2012-2014 drought. (Williams et al. 2015).

Historical Impacts

Changes detected in San Francisco Bay Area national parks and attributed to human climate change Published research using field data from the national parks has detected ecological changes statistically significantly different from historical variation and attributed the cause of those changes to human climate change more than other factors.

Sea level rise The NOAA tidal gauge hosted by Golden Gate NRA on a pier off Crissy Field is the tidal gauge with the longest time series on the U.S. west coast, with continuous readings since 1897 (Bromirski et al. 2003). Combined with previous readings from Fort Point NHS starting in 1854, the measurements show that sea level has increased 22 ± 1 cm (9 ± 0.4 in.) from 1854 to 2016 (Figure 6). This tide gauge has contributed to global analyses that have detected a statistically significant rise in global sea level from 1901 to 2010 and have attributed the rise to human climate change (Church and White 2011, IPCC 2013).

Bird range shifts Analyses of Audubon Christmas Bird Count data across the U.S., including count circles in southern Marin County and in Point Reyes NS, detected a northward shift of winter ranges of a set of 254 bird species at an average rate of 0.5 ± 0.3 km per year from 1975 to 2004, attributable more to global human climate change than local human factors (La Sorte and Thompson 2007). Further analyses demonstrate poleward shifts in winter distributions of six raptor species found in San Francisco Bay Area national parks: (American Kestrel (*Falco sparverius*), Golden Eagle (*Aquila chrysaetos*), Northern Harrier (*Circus cyaneus*), Prairie Falcon (*Falco mexicanus*), Red-tailed Hawk (*Buteo jamaicensis*), and Rough-legged Hawk (*Buteo lagopus*)) (Paprocki et al. 2014).

Changes detected in the region and attributed to human climate change Published research using field data from California has detected ecological changes statistically significantly different from historical variation and attributed the cause of those changes to human climate change more than other factors.

Wildfire Multivariate analysis of wildfire across the western U.S. from 1916 to 2003, using

data from chaparral along the entire California coast, indicates that climate was the dominant factor controlling the extent of burned area, even during periods of active fire suppression (Littell et al. 2009). The climate factors for chaparral included the Palmer Drought Severity Index (an index that combines temperature and precipitation), summer precipitation, and spring temperature two years prior to the fire. Reconstruction of fires of the past 400 to 3000 years in the western U.S. (Marlon et al. 2012, Trouet et al. 2010), including charcoal data from a pond on the Coast Trail in Point Reyes NS (Marlon et al. 2012), confirm that temperature and drought are the dominant factors explaining fire occurrence.

Sea surface temperature increase Measurements of sea surface temperatures from buoys off the California coast and around the world, combined with remote sensing data, have found warming of the top 75 m of ocean water at a rate of 1.1 ± 0.2ºC (2 ± 0.4ºF.) per century from 1971 to 2010 (IPCC 2013).

Ocean acidification Increased atmospheric carbon dioxide (CO_2) concentrations from human activities have increased the acidity of ocean water around the world by 0.1 pH units since ~1750 (IPCC 2013). This occurs when CO_2 dissolves in water and forms carbonic acid.

Changes consistent with, but not formally attributed to, human climate change Other research has examined observations consistent with, but not formally attributed to, human climate change. Some changes have only been observed and not detected (not shown statistically significantly different than historical variability).

Vegetation shifts Comparison of herbarium records for 4426 California plant species between the periods 1895-1970 and 1971-2009 found that 12% of endemic species and 27% of non-native species shifted upward in elevation (Wolf et al. 2016).

Bottlenose dolphin The southern California population of bottlenose dolphins (*Tursiops truncatus*) expanded northward into the waters off central California after the 1982-83 El Niño (Wells et al. 1990). Since then, bottlenose dolphins have been consistently sighted as far north as San Francisco, including the waters off Golden Gate NRA (Largier et al. 2011).

Harmful algal blooms When colonies of algae grow out of control, they can cover extensive areas in harmful blooms. Observations indicate increased occurrence of harmful algal blooms along the West Coast of the U.S. in the past decade (Lewitus et al. 2012). Harmful algal blooms can produce toxins that can kill people who eat tainted shellfish (Moore et al. 2008) and kill California sea lions (*Zalophus californianus*) (Scholin et al. 2000). Warmer water temperatures can contribute to formation of harmful algal blooms (O'Neil et al. 2012).

Future Climate Projections

IPCC has coordinated research groups to project possible future climates under four defined greenhouse gas emissions scenarios, called representative concentration pathways (RCPs; Moss et al. 2010). The four emissions scenarios are RCP2.6 (reduced emissions from increased energy efficiency and installation of renewable energy), RCP4.5 (low emissions), RCP6.0 (high emissions, somewhat lower than continued current practices), and RCP8.5 (highest emissions due to lack of emissions reductions).

If the world does not reduce emissions from power plants, cars, and deforestation by 40-70%, GCMs project substantial warming and slight increases in precipitation. The temperature and precipitation projections from 33 GCMs form a cloud of potential future climates (Figures 7-9). GCMs project potential increases in annual average temperature within park boundaries double to quadruple historical 20th century warming by 2100 (Tables 1, 2, 9, 11, 13). Models project the greatest temperature increases in autumn (Tables 9, 11, 13).

Because of the coarse spatial resolution of the GCMs, projected temperature increases do not show much spatial variation across the parks (Figure 10). In general, projected temperature changes increase with distance from the Pacific coast.

The average of the ensemble of GCMs projects increased precipitation under all emissions scenarios (Tables 1, 2, 10, 12, 14). The average of the ensemble reflects the central tendency of the projections, but the range of all the models can be large. In the case of the San Francisco Bay Area, two-thirds of the GCMs project increases and the rest project decreases (Figures 7-9). Projected precipitation increases tend to decrease with distance from the Pacific but do not show much spatial variation across the parks (Figure 11). Models do not project any major

changes to the temporal distribution of precipitation throughout the year (Tables 10, 12, 14).

Even if precipitation increases, temperature increases may overcome any cooling effects, leading to increased evapotranspiration and increased aridity, expressed as increased climate water deficit (difference between precipitation and actual evapotranspiration) and decreased soil moisture. Modeling of climate water deficit with one GCM under high emissions projects more arid conditions by 2100 AD in the San Francisco Bay Area (Thorne et al. 2015).

Hotter temperatures caused by human climate change have increased the probabilities of drought through increased probabilities of high temperature and low precipitation co-occurring in a single year (Diffenbaugh et al. 2015). Under the highest emissions scenario, additional warming may increase the probability that, by 2030, any annual dry period co-occurs with drought-level heat (Diffenbaugh et al. 2015).

Projections indicate potential changes in the frequency of extreme temperature and precipitation events. For northern California, under the highest emissions scenario, models project up to 10 more days per year with a maximum temperature >35ºC (95ºF.) and an increase in 20-year storms (a storm with more precipitation than any other storm in 20 years) to once every five to six years (Walsh et al. 2014).

Future Vulnerabilities

With continued emissions from power plants, cars, and deforestation, continued climate change could increase the vulnerability of park resources (IPCC 2013). Published research in the San Francisco Bay Area national parks or research that included the region has identified numerous vulnerabilities.

Terrestrial Ecosystems

Coast redwood Coast redwood (*Sequoia sempervirens*) depends on coastal fog in the summer to provide water for survival and growth. Analyses of 1895-2010 PRISM climate variables and matching of climate projections for 2020-2030 to analogous historical climate anomalies indicates that increased climate water deficit could reduce suitable climate for coast redwood in Muir Woods NM under scenarios of increased aridity (Fernandez et al.

2015).

Analysis of cloud ceiling heights along the California coast from 1951 to 2008, land temperatures from 1957 to 2008, and sea surface temperatures from 1901 to 2008 indicates a decrease of fog throughout the range of coast redwoods (Johnstone and Dawson 2010). Monitoring of leaf wetness and sap flow in a grove north of Muir Woods NM demonstrates how fog protects coast redwood from drought stress, indicating vulnerability to drought if climate change reduces fog (Johnstone and Dawson 2010). Tree-ring chronologies for the past 1700 years of coast redwoods, including five trees in Samuel P. Taylor State Park, adjacent to Muir Woods NM, showed a latitudinal gradient of climate sensitivities, with radial growth increasing with decreasing summer cloudiness in northern California forests and radial growth negatively correlated with dry summer conditions and historic fires at the southern end of the coast redwood range at Big Sur, south of the San Francisco Bay Area (Carroll et al. 2014).

Monitoring of coast redwood and sudden oak death disease before and after two wildfires in Big Sur found synergistic increases in mortality when fire and disease co-occurred, with mortality increasing as much as fourfold (Metz et al. 2013).

Vegetation and drought The canopy water content of forests across California, estimated from high-fidelity imaging spectroscopy and light detection and ranging (Lidar) scanning (Asner et al. 2016), reveals how the 2012-2014 drought dried and killed trees. In August 2015, remote sensing found high canopy water content (~4 L per square meter) in Muir Woods NM, low canopy water content (~0.5 L per square meter) in Point Reyes NS, and medium levels (0.5 to 2 L per square meter) in Golden Gate NRA (Asner et al. 2016). Projected increases of climate water deficit across the San Francisco Bay Area (Thorne et al. 2015) could increase drought stress of vegetation. In California, more non-native plant species may shift upward than endemic plant species (Wolf et al. 2016). The perennial ferns *Polystichum munitum* and *Dryopteris argute*, found in the understory of coast redwood, are adapted to water stress of the magnitude experienced in the California 2012-2014 drought, when they experienced extensive dieback but recovered after substantial rains (Baer et al. 2016).

Vegetation shifts Modeling of 22 major vegetation types in the San Francisco Bay Area based on climate and soil factors indicates that, under a range of climate change projections, chamise chaparral may tend to replace coastal scrub and grassland in Golden Gate NRA and Point Reyes NS (Ackerly et al. 2015). Vegetation modeling on coastal scrub at Point Reyes NS indicated that it is vulnerable to range contraction due to climate change (Hameed et al. 2013). Other modeling of the 29 major vegetation types across the State of California under climate change shows only moderate vulnerability to range changes in San Francisco Bay Area parks (Thorne et al. 2016).

Rare plant species An assessment of life history attributes and species distribution models of 156 rare plant species in California identified 42 species as extremely or highly vulnerable to a reduction in population due to climate change (Anacker et al. 2013). Two of these species are found in Golden Gate NRA and Point Reyes NS: California bedstraw (*Galium californicum*) and San Francisco owl's clover (*Triphysaria floribunda*). Two others are found only in Point Reyes NS: coast lily (*Lilium maritimum*) and Welsh mudwort (*Limosella australis*), a plant listed as endangered under the Endangered Species Act and ranked by Anacker et al. (2013) as one of the five most vulnerable plant species in California

Wildfire Under high emissions, climate change may increase potential burned area 50% to 100% in Point Reyes NS and in some parts of Golden Gate NRA south of the Golden Gate by 2085 (Westerling et al. 2011).

Invasive plant species Exotic grass species are generally annual, taller, with larger leaves, and larger seeds than native species. Across California, these traits are associated with higher temperature and exotic grass species are more dominant in warmer areas of the state (Sandel and Dangremond 2012). Under warming conditions, more non-native plant species in California may shift upward than endemic plant species (Wolf et al. 2016). Under high emissions, the region would continue to provide suitable habitat for the invasive yellow starthistle (*Centaurea solstitialis*) (Bradley et al. 2009), common in John Muir NHS.

Birds An assessment of 358 vertebrate taxa in California listed numerous bird species in

Golden Gate NRA and Point Reyes NS as highly vulnerable to drought, a possible vulnerability under climate change (California Department of Fish and Wildlife 2016): American white pelican (*Pelecanus erythrorhynchos*), black tern (*Chlidonias niger*), California black rail (*Laterallus jamaicensis coturniculus*), harlequin duck (*Histrionicus histrionicus*), redhead (*Aythya americana*), tricolored blackbird (*Agelaius tricolor*), western snowy plover (*Charadrius nivosus nivosus*; listed as threatened under the Endangered Species Act), willow flycatcher (*Empidonax traillii*; listed as endangered under the Endangered Species Act), and yellow rail (*Coturnicops noveboracensis*). The least bittern (*Ixobrychus exilis*), found in Point Reyes NS, was also listed as highly vulnerable to drought. The western snowy plover is also vulnerable to losing habitat as sea level inundates more of its coastal habitat (Hutto et al 2015).

An assessment of 358 California bird species (Gardali et al. 2012) judged 128 vulnerable to climate change, but the northern spotted owl (*Strix occidentalis caurina*) was judged not vulnerable. Field research from 1985 to 1994 on northern spotted owls in Humboldt County, California, found that temperature and precipitation explained observed recruitment, reproduction, and survival more than habitat factors (Franklin et al. 2000). Survival increased with increasing temperature and decreasing precipitation.

Field research from 1985 to 2013 on northern spotted owls in Washington, Oregon, and California north of the San Francisco Bay Area found that recruitment was most highly correlated to low winter temperature and precipitation (Dugger et al. 2016). Field studies and modeling of northern spotted owls in Oregon and Washington found that warmer, wetter winters and hotter, drier summers, could decrease owl survival (Glenn et al. 2011).

Amphibians and Reptiles An assessment of 358 vertebrate taxa in California listed one amphibian and two reptile species in Golden Gate NRA as highly vulnerable to drought, a possible vulnerability under climate change (California Department of Fish and Wildlife 2016): California red-legged frog (*Rana draytonii*; listed as threatened under the Endangered Species Act), pond turtle (*Emys marmorata*), and San Francisco garter snake (*Thamnophis sirtalis tetrataenia*; listed as endangered under the Endangered Species Act).

Aquatic Ecosystems and Coastal Infrastructure

Sea level rise If the world does not reduce emissions from power plants, cars, and deforestation, climate change could continue to raise sea level globally through two mechanisms: (1) expansion of ocean water when it warms and (2) increased volume of water in the oceans from meltwater from glaciers and ice on land.

Two different analyses provide future sea level projections for the San Francisco Bay Area. In the older of the two analyses (NRC 2012), a panel of the National Academy of Sciences of the USA combined data from two sources: (1) ocean thermal expansion projections from process-based models, published in 2007 by the Intergovernmental Panel on Climate Change (IPCC) (IPCC 2007) and using the greenhouse gas emissions scenarios developed in 2000 (IPCC 2000), and (2) the panel's extrapolation of land ice melting from glaciers, ice caps, Greenland, and Antarctica. In the newer of the two analyses (IPCC 2013), IPCC used process-based models (computer models of physical processes, calibrated using field measurements) for ocean thermal expansion and for land ice melting from glaciers, ice caps, Greenland, and Antarctica, using updated emissions scenarios developed in 2010 (Moss et al. 2010). IPCC (2013) projections employ more updated methods and data.

The older analyses projected sea level rise for the West Coast of the U.S. of 40 cm (16 in.) for a low emissions scenario and 170 cm (67 in.) for the highest emissions scenario by 2100 AD (NRC 2012). The newer analyses projected global sea level rise of 26-55 cm (10-22 inches) for the lowest emissions scenario and 52-98 cm (20-39 inches) for the highest emissions scenario by 2100 AD (IPCC 2013). Maps of the spatial variation of global sea level rise projections indicate sea level rise for the San Francisco Bay Area similar to the global average (IPCC 2013).

Analyses of the vulnerability of the coasts of Golden Gate NRA and Point Reyes NS to physical change has analyzed relative sea level change, mean wave height, geomorphology, historical shoreline change, regional coastal slope, and mean tidal range for 1.7 km long segments of shoreline (Pendleton et al. 2010). Approximately half of the shoreline in both parks show high vulnerability (Figures 12, 13). In general, shorelines with

rock cliffs, steep slopes, and low wave heights are less vulnerable.

Storm surge would occur over and above the projected sea level rise, with models projecting more frequent and intense coastal flooding. NPS research on combined projections of sea level rise, using the IPCC (2013) projections, and storm surge in Golden Gate NRA and Point Reyes NS is in progress by Dr. Maria Caffrey, University of Colorado.

The major future vulnerability to sea level rise is the direct inundation of land. In Golden Gate NRA, sea level rise of 1 m could inundate one-fifth of the 75 ha of land around Stinson Beach (Hoover et al. in press). At Crissy Field, sea level rise by 2100 AD of 1 m above the current high water level (Mean Higher High Water, average of the higher high water height of each tidal day observed from 1983 to 2001, occurring approximately 50 times a year) could flood extensive areas of the marsh and inundate many buildings and other infrastructure (Figure 14; CMG 2016). The projected area of flooding under that scenario, which could occur 50 times a year, is approximately equivalent to the flooding from a current 100-year tide, the water level that statistically occurs once in 100 years.

Analyses of elevation data indicate high exposure of major infrastructure in San Francisco Bay Area national parks to 1 m sea level rise, including Fort Point, the core resource of Fort Point NHS; Piers 2, 3, and 4, the Alcatraz waterfront, the Crissy Field channel bridge, and numerous trails and buildings in Golden Gate NRA; the Estero Trail, Historic Lifeboat Station Boathouse, and other buildings at Point Reyes NS; and the Aquatic Park Municipal Pier and other docks and buildings in the San Francisco Maritime NHP (Peek et al. 2015).

In Point Reyes NS, sea level rise, storm surge, and coastal erosion threaten to damage Indian archaeological sites along cliff edges next to open ocean, in inland tidal areas, and on the coast (Newland 2013).

In Point Reyes NS and Golden Gate NRA, sea level rise threatens to inundate habitat for the western snowy plover (*Charadrius nivosus nivosus*; listed as threatened under the Endangered Species Act), harbor seals (*Phoca vitulina*) (Largier et al. 2011), and Northern elephant seals (*Mirounga angustirostris*) (Funayama et al. 2013).

Ocean acidification Under high emissions, ocean acidification can dissolve the shells of many marine species and deplete near-shore waters of calcium carbonate for almost all of the year (Gruber et al. 2012), rendering vulnerable many marine species. Acidity reduces the water concentrations of calcium carbonate that many marine species, including pteropods, shellfish, and corals, require for building shells for survival.

California Current changes Intensification of winds under climate change could increase upwelling in the California Current system under climate change (Garcia-Reyes et al. 2010, Sydeman et al. 2014), which could increase nutrient inputs into surface waters, disrupt food webs, and alter diet composition of marine birds (Sydeman et al. 2001). Models under very high emissions, however, do not agree on projections of changes in the California Current (Wang et al. 2015).

San Francisco Bay salinity San Francisco Bay is vulnerable to increased salinity under climate change. Projected warmer winter temperatures in the Sierra Nevada could decrease winter snowpack, increase winter runoff, decrease spring and summer runoff, reduce spring and summer fresh water inflows into San Francisco Bay, and increase salinity in the Bay 3 to 5 g per kg of water by 2100 AD (Cloern et al. 2011, Knowles and Cayan 2002, 2004).

Inland streams Models do not project any major changes to the temporal distribution of precipitation in Golden Gate NRA, Muir Woods NM, and Point Reyes NS throughout the year, indicating little change in the timing of streamflow (Tables 10, 12, 14). Under one general circulation model projection of decreased precipitation, a hydrological model projects reduced runoff and groundwater recharge in the San Francisco Bay Area (Thorne et al. 2015).

Marine mammals Gray whales (*Eschrichtius robustus*), which migrate through the waters of Point Reyes NS and off the coast of Golden Gate NRA, may spend more time in Arctic waters due to longer and earlier ice-free conditions, changing the timing and duration of their passage through California waters (Moore and Huntington 2008). Ocean temperatures also affect distributions of California sea lion (*Zalophus californianus*), harbor porpoise (*Phocoena phocoena*), and other marine mammals in the California Current system (Keiper

et al. 2005) and in haul-outs and rookeries in Point Reyes NS (Sydeman and Allen 1999). Northern elephant seals (*Mirounga angustirostris*) are vulnerable to losing breeding ground and haul-out space in Point Reyes NS due to sea level rise (Funayama et al. 2013).

Intertidal invertebrate range shifts Resurvey of a 1931-1933 intertidal transect of mollusks, snails, and other invertebrates in Monterey Bay in the period 1993-1996 found that 10 of 11 southern species increased and five of seven northern species decreased as sea surface temperatures increased (Barry et al. 1995, Sagarin et al. 1999). This suggests vulnerability of Duxbury Reef and other intertidal areas in Point Reyes NS and Golden Gate NRA to northward range shifts of invertebrates.

Fish Warming of river and stream waters due to climate change could contribute to possible extirpation from California of coho salmon (*Oncorhynchus kisutch*) and steelhead (*Oncorhynchus mykiss*) (Katz et al. 2013). Projections under high emissions of the ranges of 28 North Pacific fish species, including coho salmon and steelhead, indicate possible shifts northward of 300 ± 20 km per century (mean ± standard error) due to warmer sea surface temperatures and loss of two or three species from the waters off Golden Gate NRA and Point Reyes NS (Cheung et al. 2015).

The tidewater goby (*Eucyclogobius newberryi*) is listed as endangered under the Endangered Species Act and is found in Golden Gate NRA at Giacomini wetland (managed by Point Reyes NS) and at Rodeo Lagoon. Observations in estuaries along the coast of California found that larval durations of tidewater goby in warmer waters were shorter, growth rates were faster, and fish were smaller at settlement, indicating vulnerability to reduced survival under climate change (Spies and Steele 2016).

Ecosystem Carbon

Growing vegetation naturally removes carbon from the atmosphere, reducing the magnitude of climate change. Conversely, deforestation, wildfire, and other agents of tree mortality emit carbon to the atmosphere, exacerbating climate change. Determining the balance between ecosystem carbon emissions to the atmosphere and removals from the atmosphere is essential for tracking the role of ecosystems in climate change (IPCC 2013). Analyses of Landsat remote sensing and field measurements of biomass across the state of California have produced

estimates of the carbon in aboveground vegetation for the grasslands, woodlands, forests, and other non-agricultural and non-urban areas of the state at 30 m spatial resolution (Gonzalez et al. 2015). Monte Carlo analyses of variation and errors in tree measurements, remote sensing, and the carbon fraction of biomass quantified the uncertainty of carbon stock change estimates. Validation of the carbon stock estimates by independent measurement-derived stocks at field sites and matching of forest carbon stock estimates with other remote sensing-derived stocks indicated the skill of the carbon estimation methods.

In 2010, aboveground live vegetation in the nine national parks contained 2 ± 1 million tons of carbon (Table 15) (Gonzalez et al. 2015). This stock is equivalent to the greenhouse gases emitted in one year by 370 000 ± 140 000 Americans. Coast redwood trees (*Sequoia sempervirens*) contain carbon at the highest carbon density in the world, 2600 ± 100 tons per hectare, in Jedediah Smith Redwoods State Park, adjacent to Redwood National Park, and a density of 970 ± 50 tons per hectare in Samuel P. Taylor State Park, adjacent to Muir Woods NM (Van Pelt et al. 2016). So, the coast redwoods in Muir Woods NM and the Phleger Estate in Golden Gate NRA have the capacity to grow to the highest carbon densities in the San Francisco Bay Area (Figure 15). Based on whole-tree measurements, redwood wood growth increases with tree size and age (Sillett et al. 2010).

From 2001 to 2010, aboveground vegetation carbon increased on 11% of the land area of the nine parks and decreased on 7% (Figure 16; Gonzalez et al. 2015). The carbon increases result from increased vegetation cover and tree height. The carbon decreases occurred due to reduced vegetation cover and tree height, due to vegetation type conversion, mortality, and fire.

Wetland ecosystems store carbon mainly in organic soils. Globally, tidal marshes contain soil organic carbon at densities of 60 to 260 tons per hectare (Pendleton et al. 2012), revealing a potential carbon side-benefit of any wetland restoration in San Francisco Bay Area national parks. Tidal wetlands in the North Bay and East Bay, outside of the national parks, accumulated soil organic carbon at a rate of 0.8 tons per hectare per year from 2009 to 2010 (Callaway et al. 2012).

Acknowledgements

Thanks to Sarah Allen, Alison Forrestel, Daphne Hatch, and Bill Merkle (National Park Service science staff in the San Francisco Bay Area) for detailed and helpful input.

Figure 1


National Parks of the San Francisco Bay Area, California
Point Reyes
National Seashore
Muir Woods
National Monument
Golden Gate
National Recreation Area
P
J
R
F
S
E
Eugene O'Neill National Historic Site (E)
Fort Point National Historic Site (F)
John Muir National Historic Site (J)
Port Chicago Naval Magazine National Memorial (P)
Rosie the Riveter WWII Home Front National Historical Park (R)
San Francisco Maritime National Historical Park (S)
10 kilometers (6 miles)
Data: USGS Landsat August 12, 2015
Cartography: P. Gonzalez

Figure 2

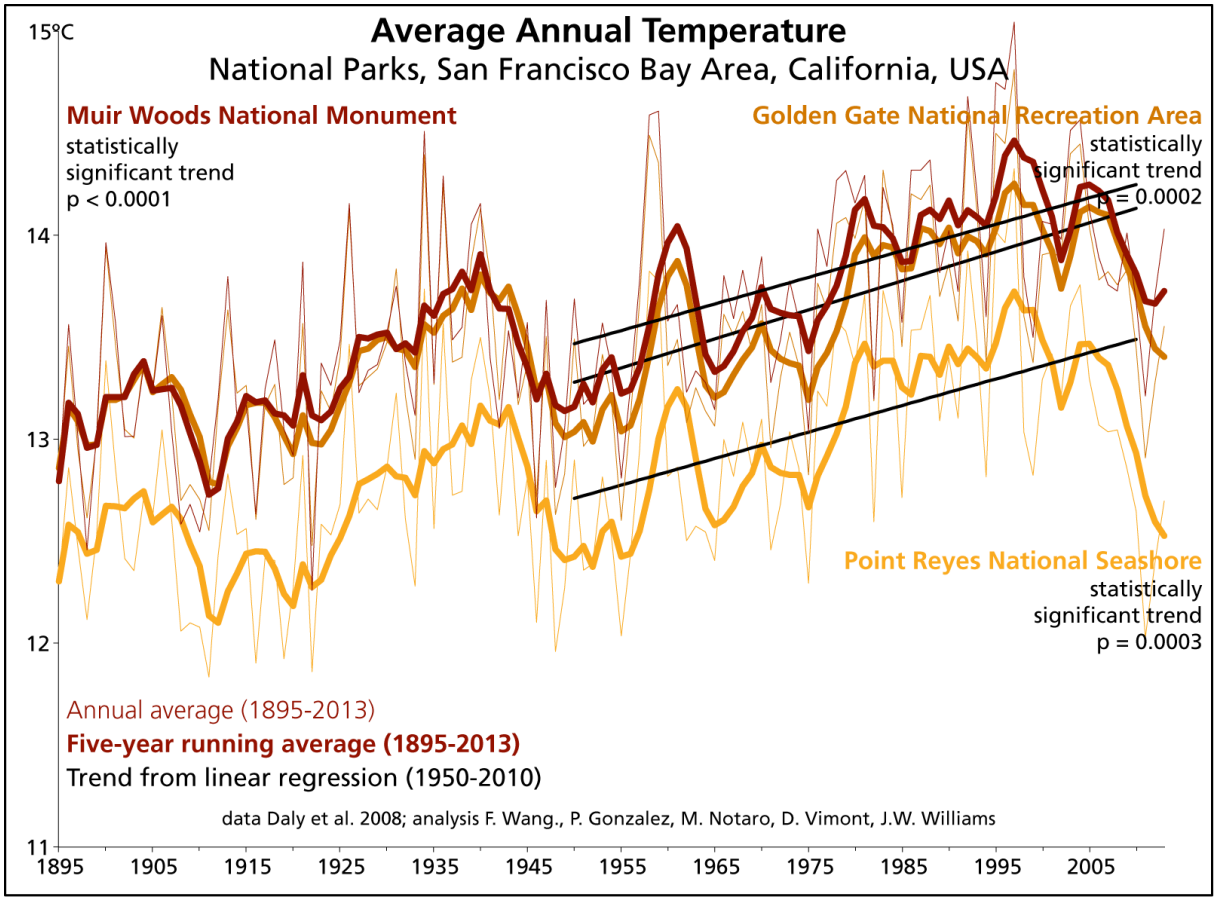

Main conclusion: Temperature has increased at statistically significant rates.

Figure 3

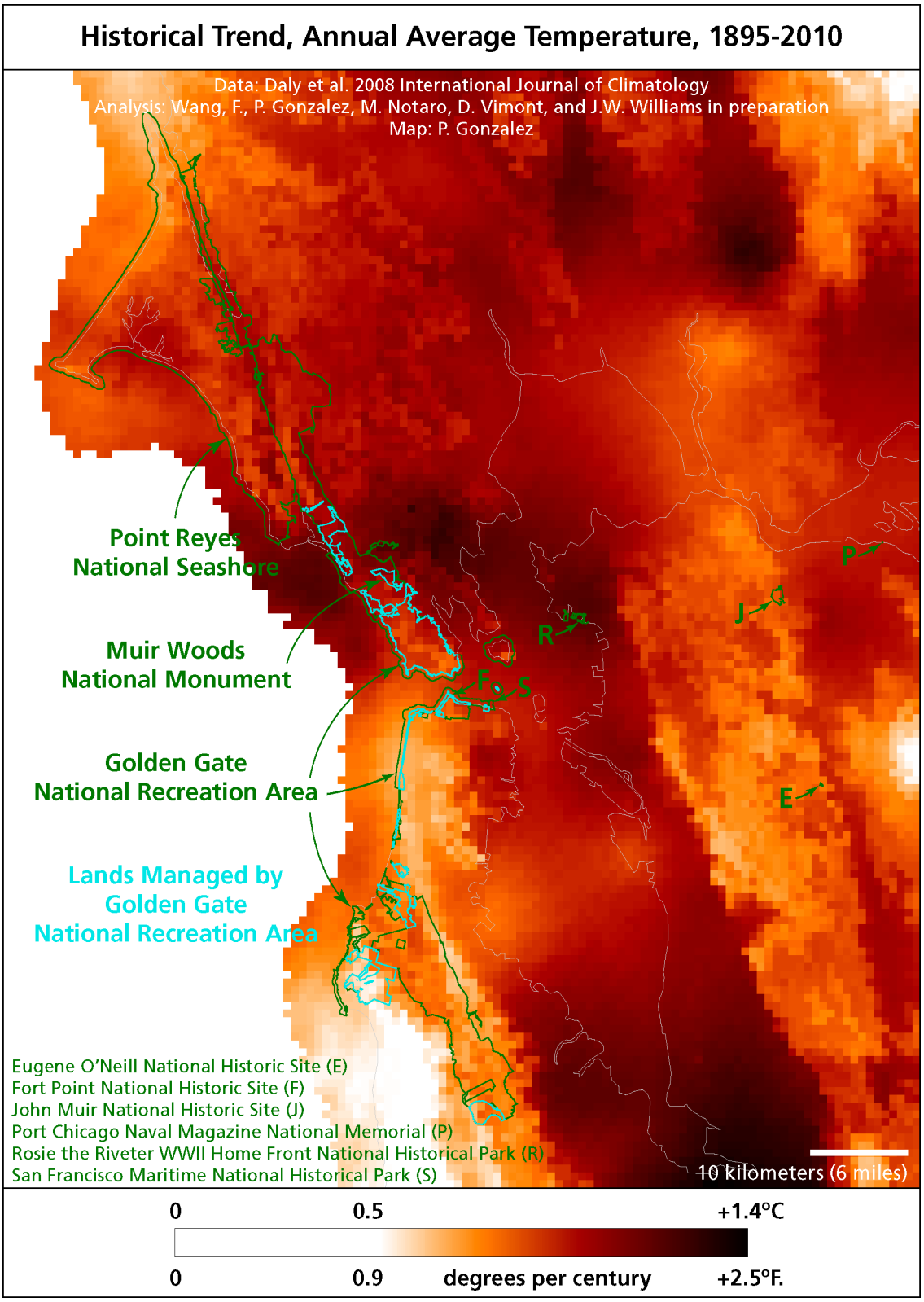

Main conclusion: Temperature increases are high north of Muir Woods NM and in the South Bay.

Figure 4

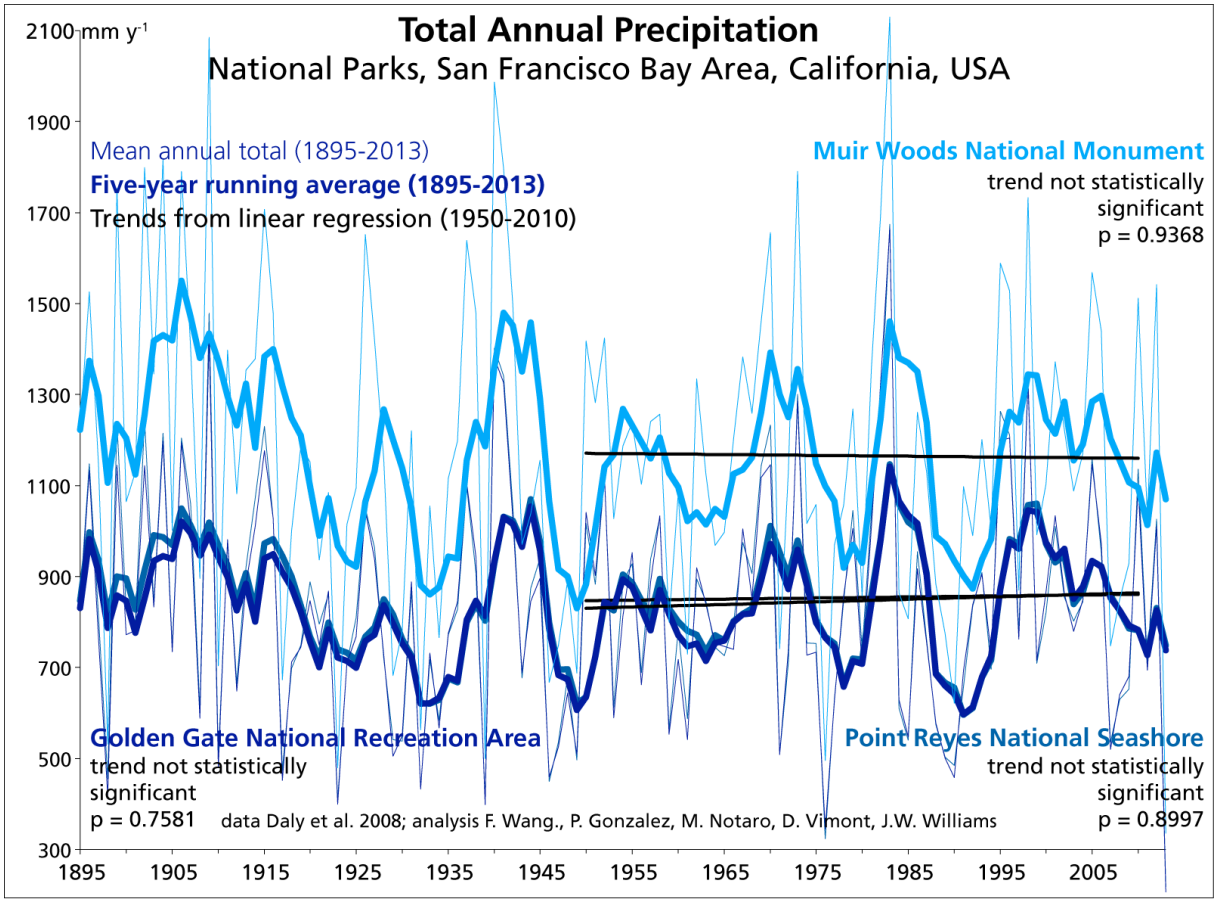

Main conclusion: Precipitation has shown no statistically significant change.

Figure 5

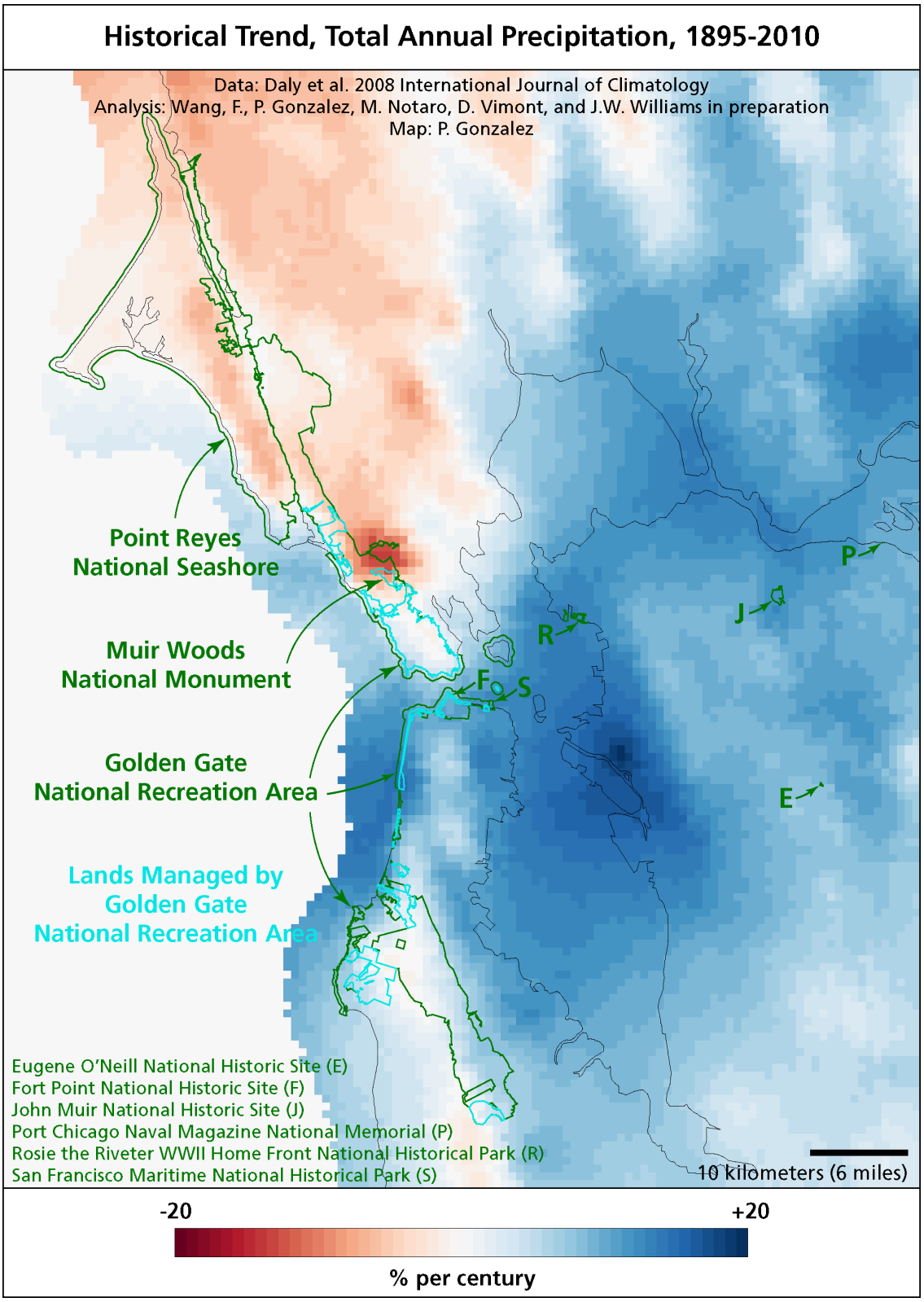

Main conclusion: Precipitation has decreased north of the Golden Gate and increased to the south.

Figure 6

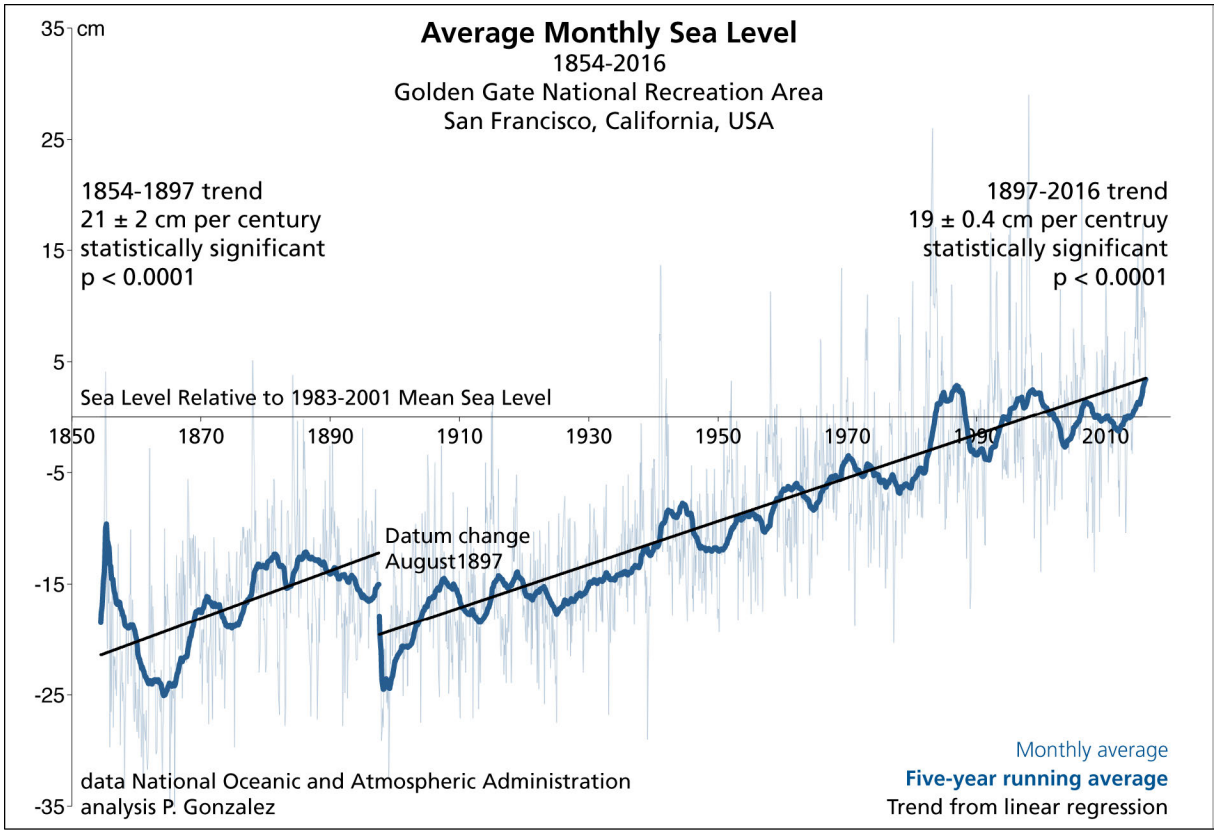

Main conclusion: Sea level has risen at a statistically significant rate since 1854.

Figure 7

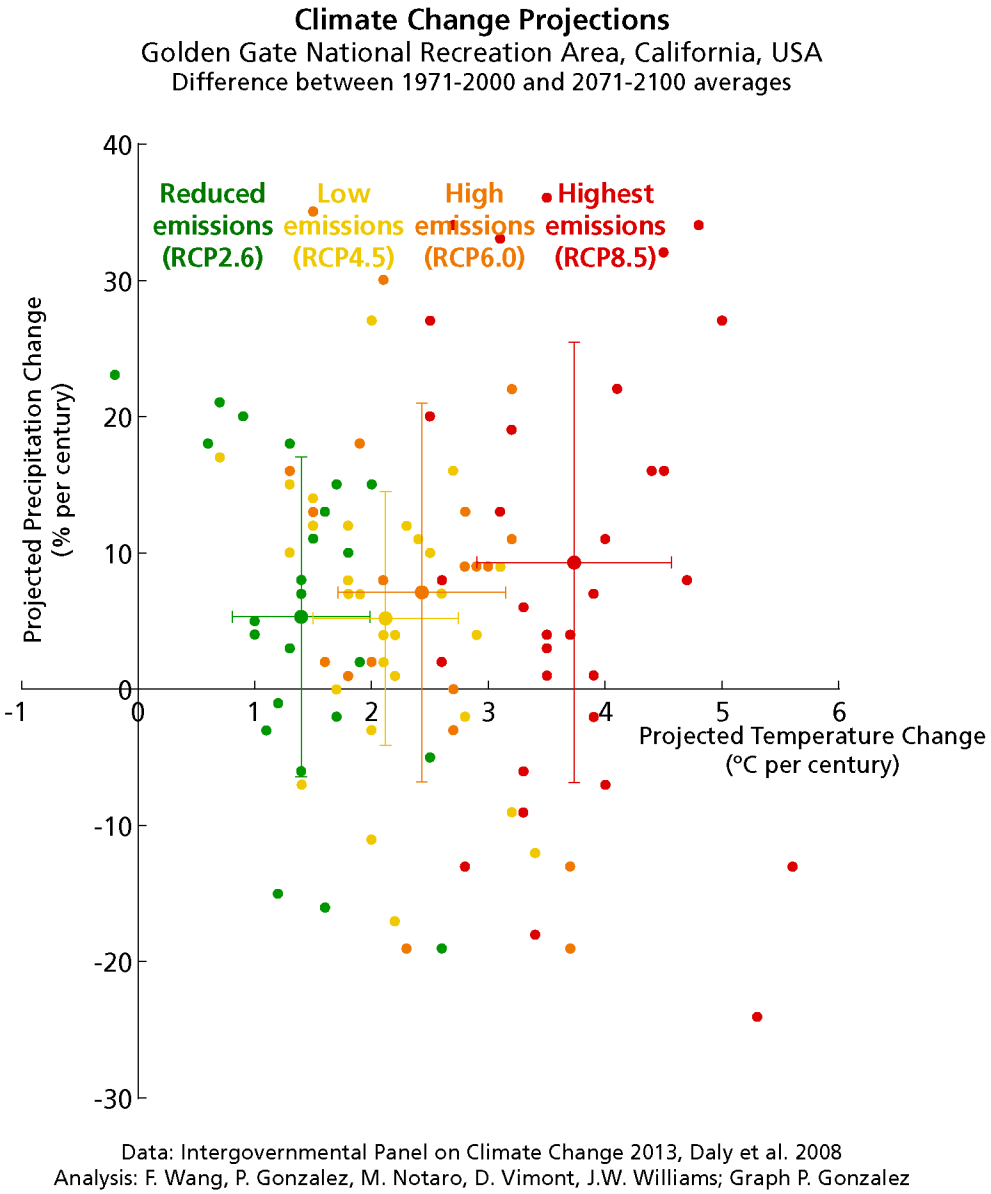

Main conclusion: All models project increased temperature and two-thirds project increased precipitation.

Projections of future climate for the area within park boundaries, relative to 1971-2000 average values. Each small dot is the output of a single GCM. The large color dots are the average values for the four IPCC emissions scenarios. The crosses are the standard deviations of each emissions scenario average. (Data: IPCC 2013, Daly et al. 2008; Analysis: F. Wang, P. Gonzalez, M. Notaro, D. Vimont, J.W. Williams).

Figure 8

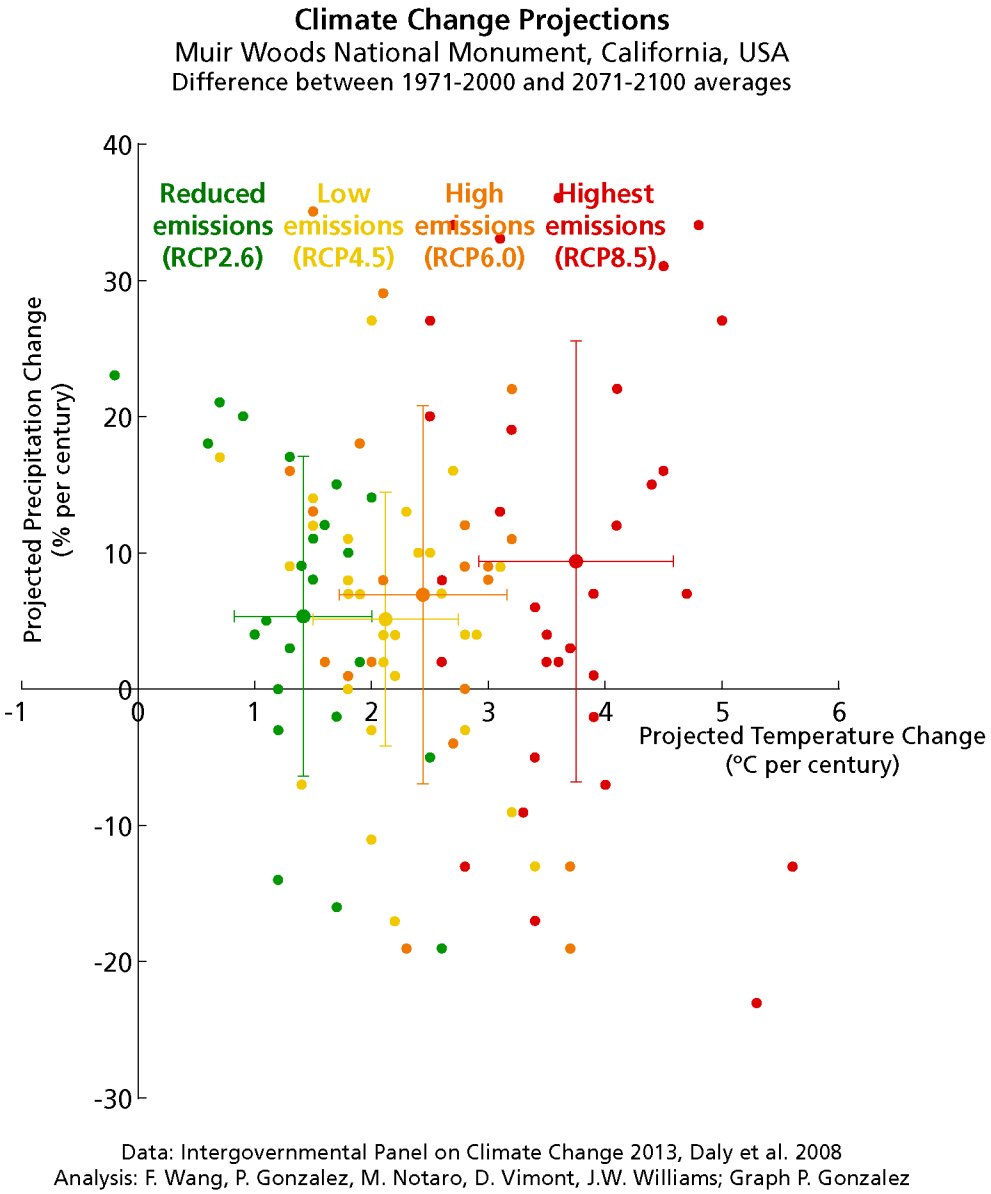

Main conclusion: All models project increased temperature and two-thirds project increased precipitation.

Projections of future climate for the area within park boundaries, relative to 1971-2000 average values. Each small dot is the output of a single GCM. The large color dots are the average values for the four IPCC emissions scenarios. The lines are the standard deviations of each emissions scenario average. (Data: IPCC 2013, Daly et al. 2008; Analysis: F. Wang, P. Gonzalez, M. Notaro, D. Vimont, J.W. Williams).

Figure 9

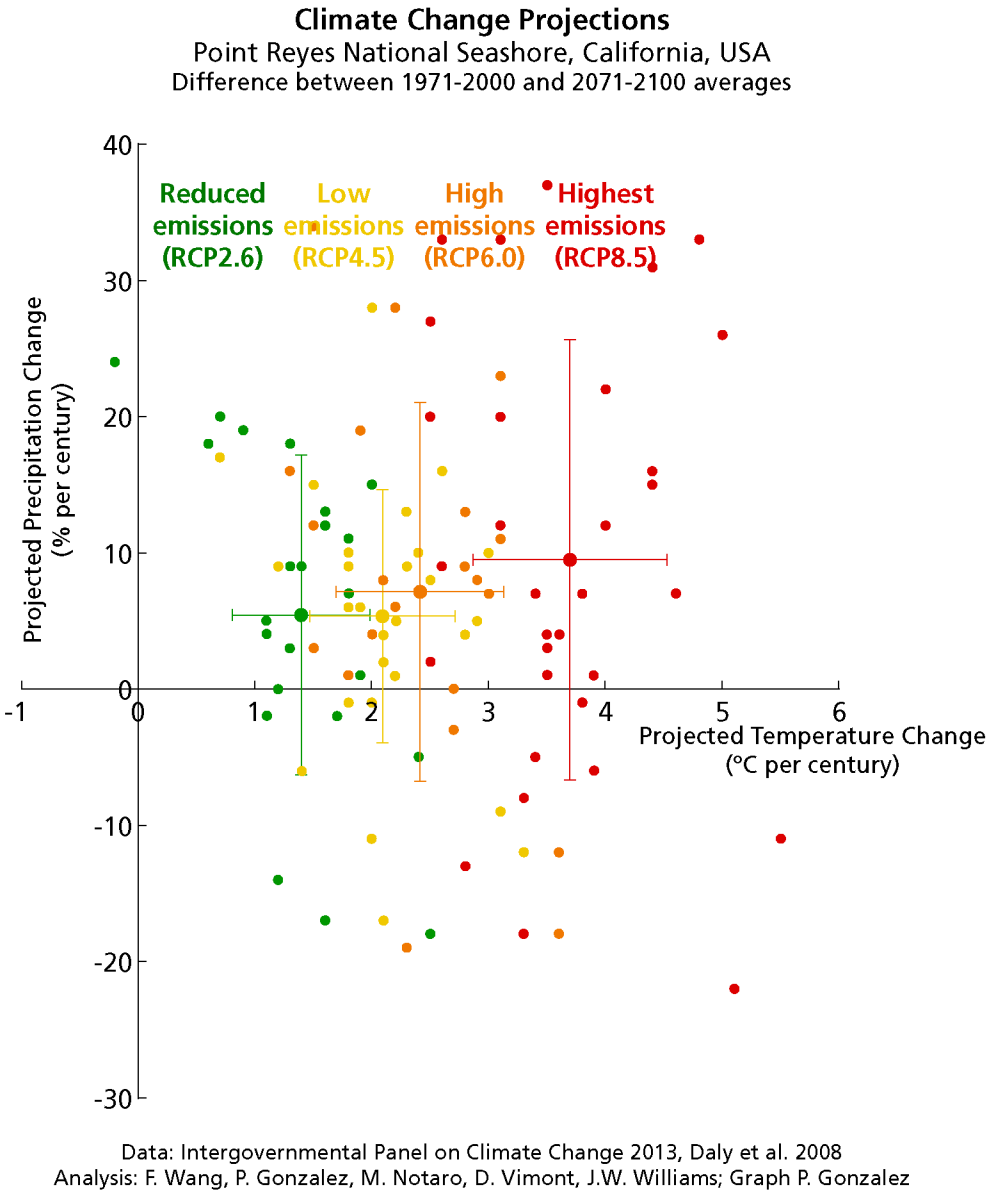

Main conclusion: All models project increased temperature and two-thirds project increased precipitation.

Projections of future climate for the area within park boundaries, relative to 1971-2000 average values. Each small dot is the output of a single GCM. The large color dots are the average values for the four IPCC emissions scenarios. The lines are the standard deviations of each emissions scenario average. (Data: IPCC 2013, Daly et al. 2008; Analysis: F. Wang, P. Gonzalez, M. Notaro, D. Vimont, J.W. Williams).

Figure 10

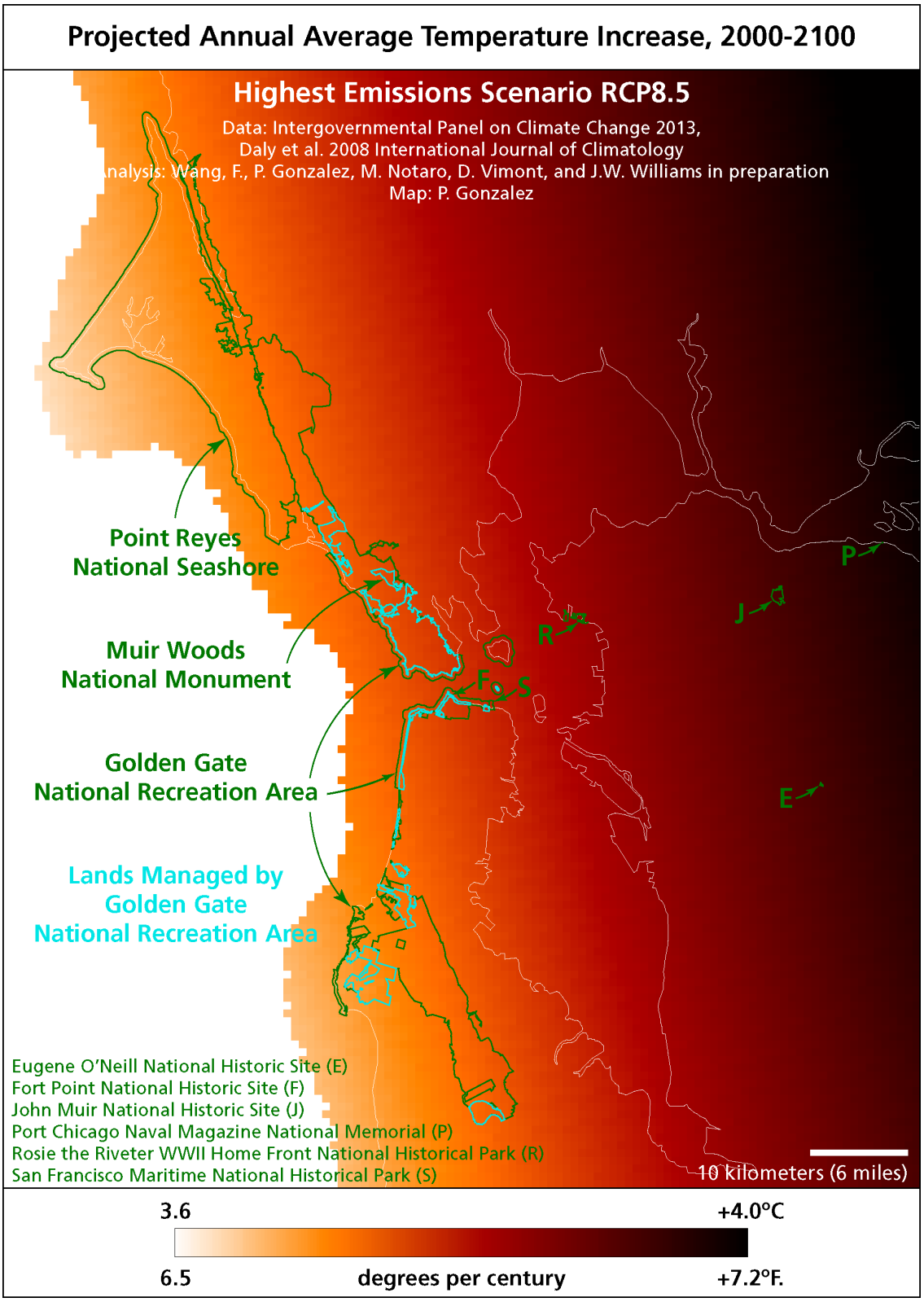

Main conclusion: Projected temperature changes increase with distance from the Pacific coast.

Figure 11

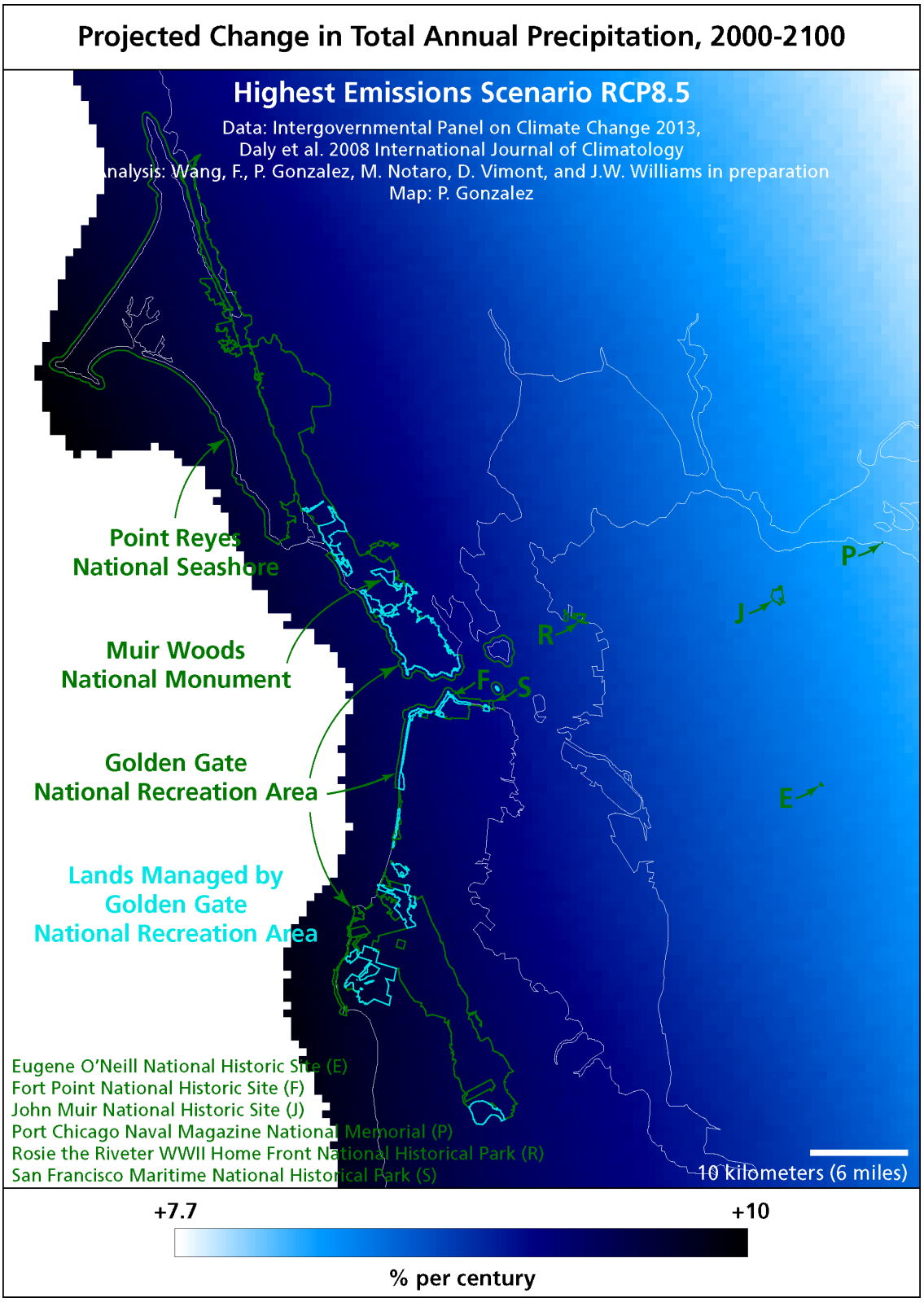

Main conclusion: Projected precipitation changes increase toward the Pacific coast.

Figure 12

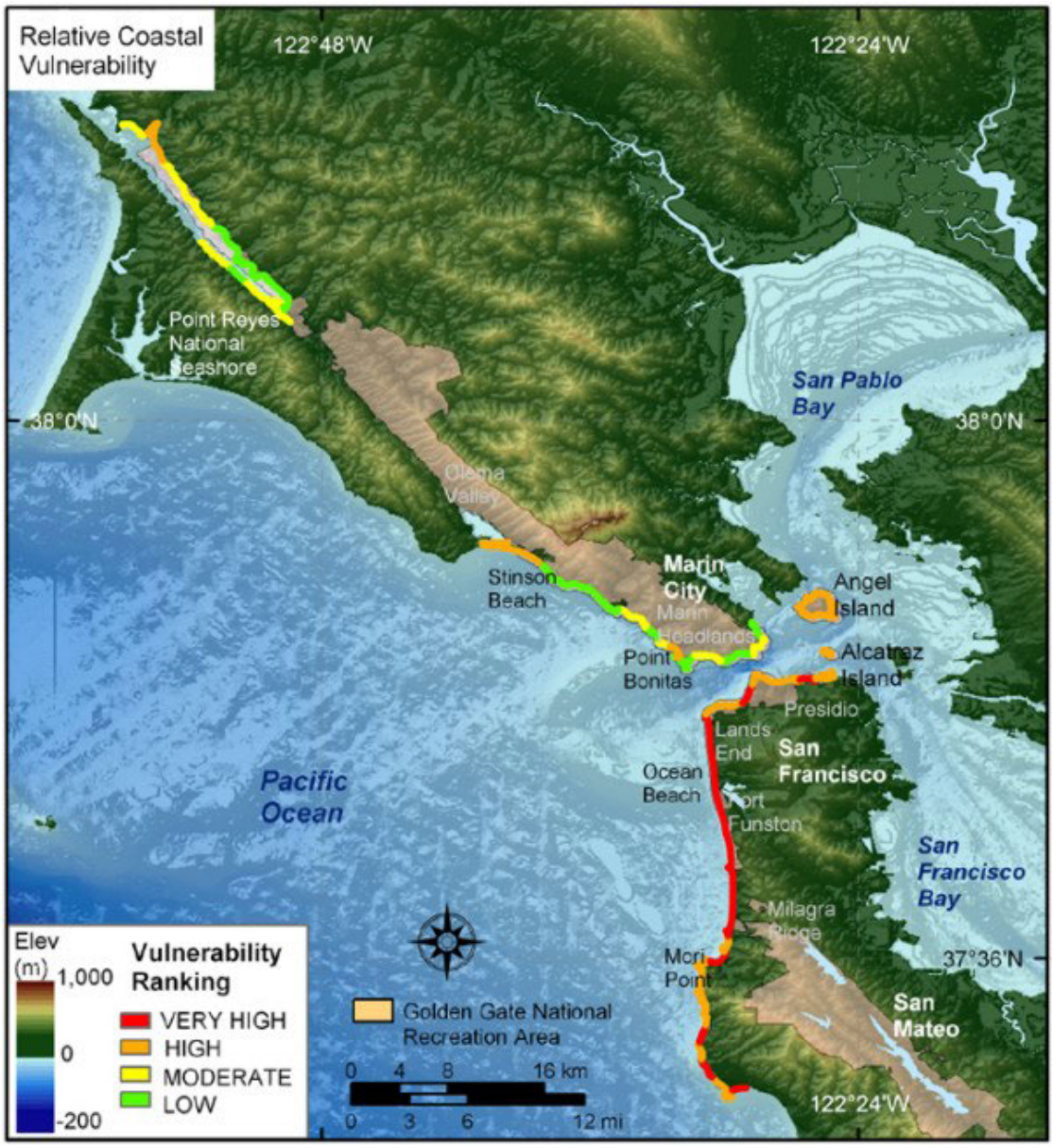

Analysis and Map: Pendleton et al. (2010)

Main conclusion: Vulnerability to sea level rise and storm surges are high to very high for half the coastline of Golden Gate NRA.

Figure 13

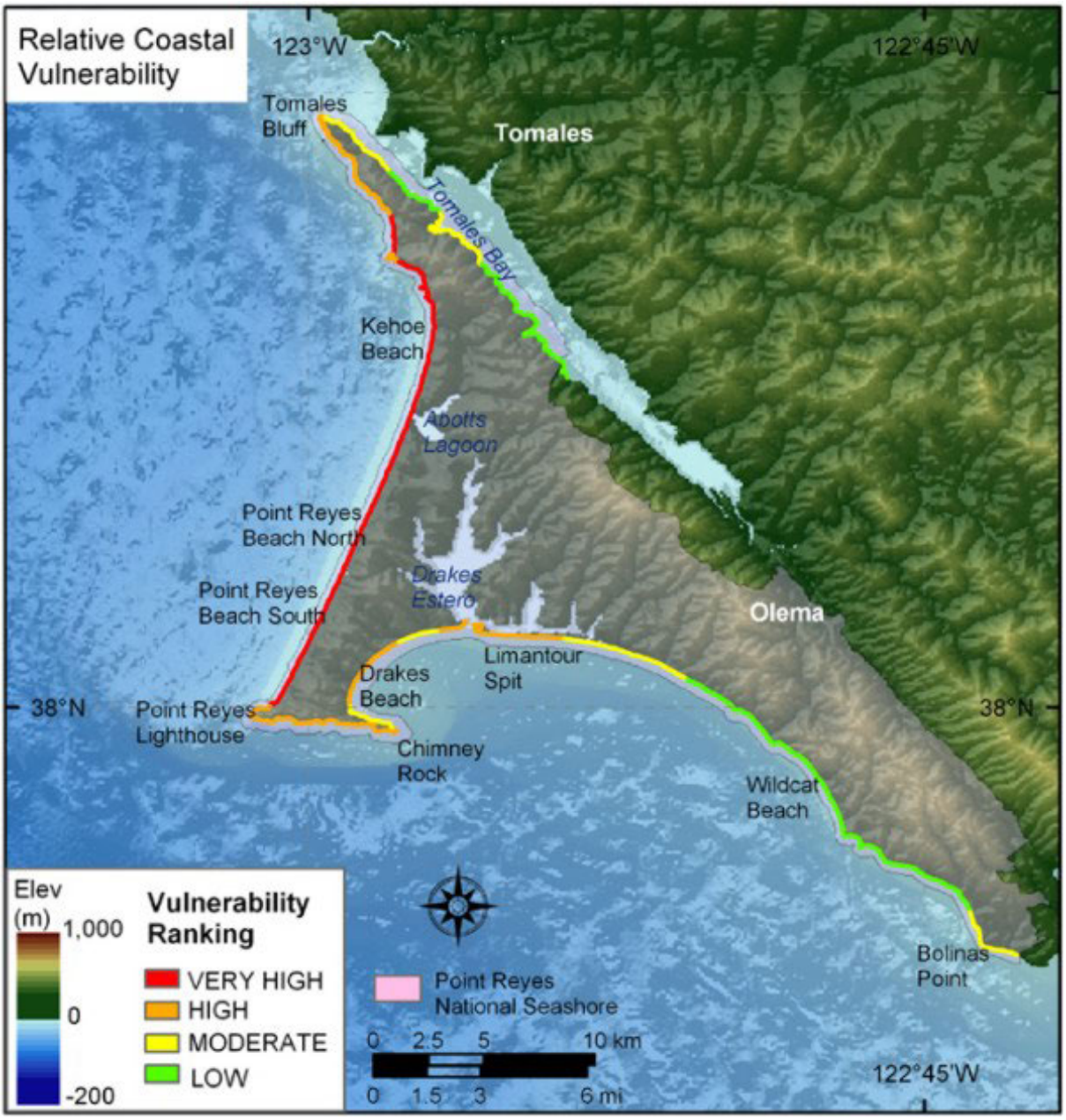

Analysis and Map: Pendleton et al. (2010)

Main conclusion: Vulnerability to sea level rise and storm surges are highest along Point Reyes beach.

Figure 14. Projected flood (dark blue areas) from sea level rise of 1 m (highest IPCC (2013) sea level rise projection) above the current high water level, which occurs approximately 50 times a year (CMG 2016).

Figure 15

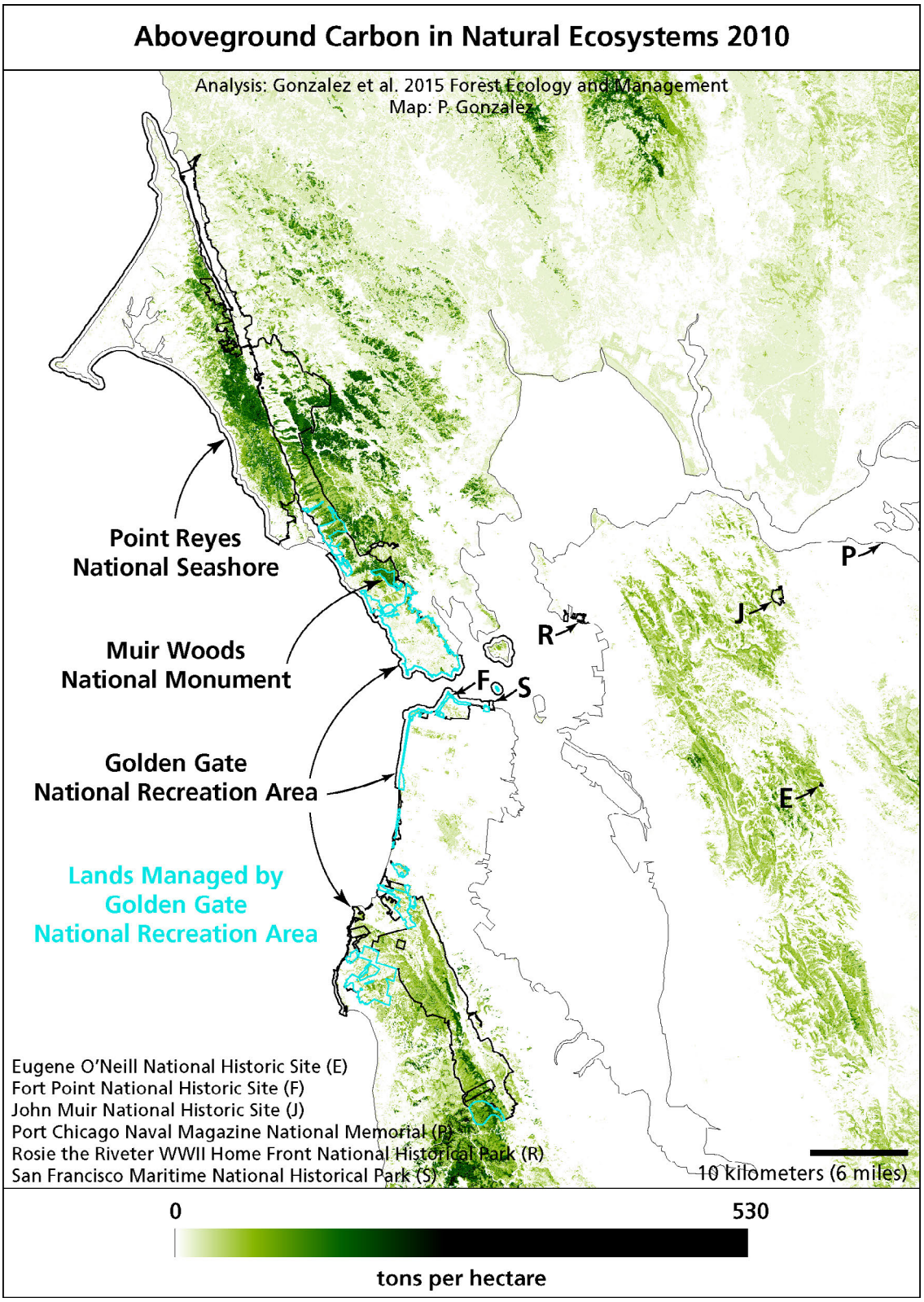

Main conclusion: Carbon densities are highest in the coast redwoods and other forests.

Figure 16

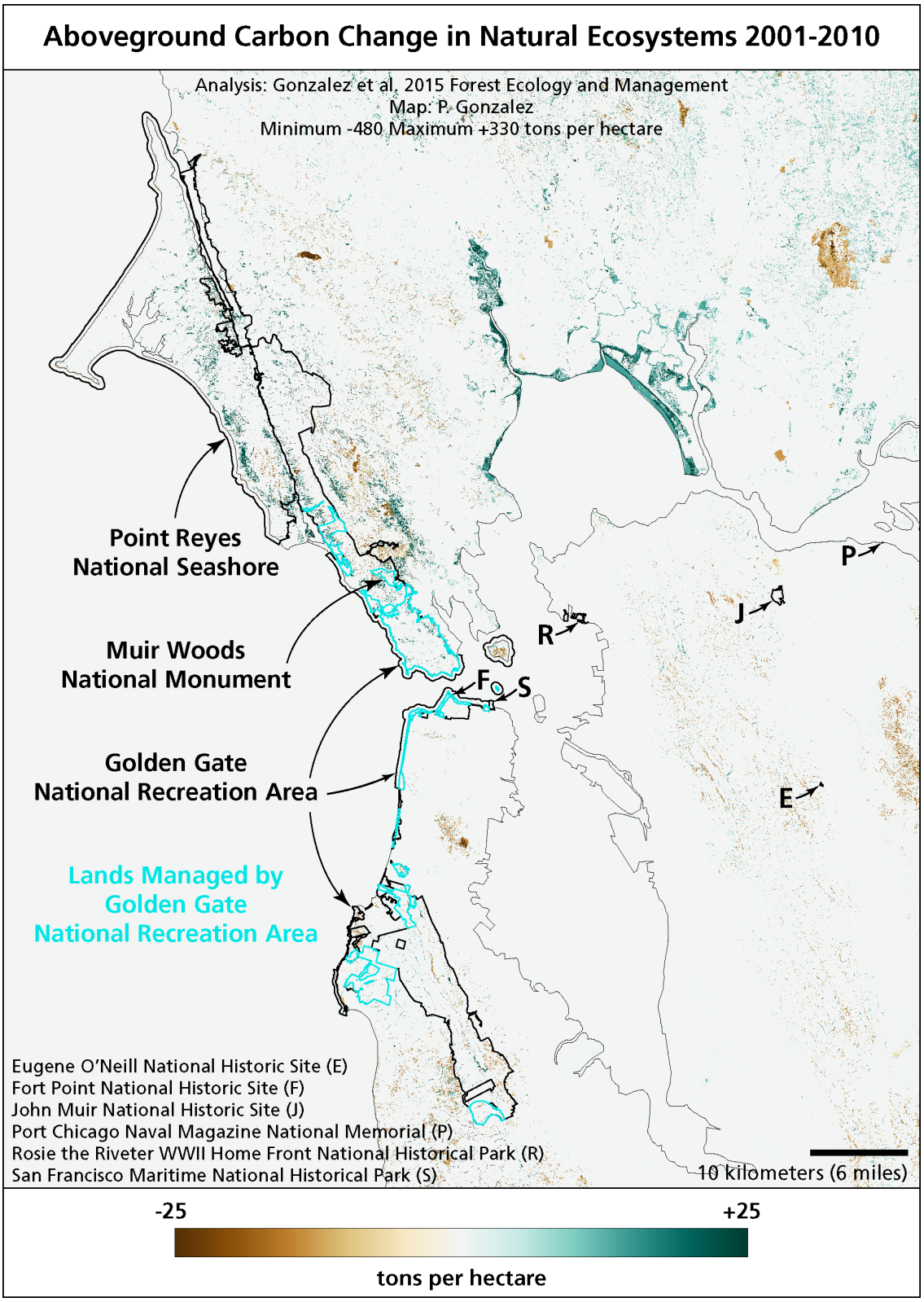

Main conclusion: Ecosystem carbon increased across wide areas in Point Reyes NS.

Table 1. **Climate Change Trends**. Historical rates of change (mean ± standard error) and projected future changes (mean ± standard deviation) in annual average temperature (ºC per century) and total annual precipitation (% per century) (data Daly et al. 2008, IPCC 2013; analysis Wang et al. in preparation). All of the historical temperature trends are statistically significant but none of the precipitation trends are. Temperatures in degrees Fahrenheit (ºF.) are approximately double the number in degrees Celsius (ºC). IPCC = Intergovernmental Panel on Climate Change, NHS = National Historic Site, NM = National Monument, NRA = National Recreation Area, RCP = Representative Concentration Pathway.

	Golden Gate NRA				Muir Woods NM	Point Reyes NS
	legislative boundary	managed area	managed north	managed south		
Historical (1895-2010)						
temperature	0.9 ± 0.2	0.7 ± 0.1	0.9 ± 0.1	0.6 ± 0.1	1 ± 0.2	0.9 ± 0.2
precipitation	1 ± 9	-1 ± 8	-3 ± 8	1 ± 8	-7 ± 9	-3 ± 9
Historical (1950-2010)						
temperature	1.4 ± 0.5	1.1 ± 0.3	1.2 ± 0.3	1.1 ± 0.3	1.3 ± 0.5	1.3 ± 0.5
precipitation	7 ± 25	-2 ± 20	-3 ± 8	1 ± 22	-2 ± 21	3 ± 25
Projected (2000-2100)						
Reduced emissions (IPCC RCP 2.6)						
temperature	1.4 ± 0.6	1.4 ± 0.6	1.4 ± 0.6	1.4 ± 0.6	1.4 ± 0.6	1.4 ± 0.6
precipitation	5 ± 12	5 ± 12	5 ± 12	5 ± 12	5 ± 12	5 ± 11
Low emissions (IPCC RCP 4.5)						
temperature	2.1 ± 0.6	2.1 ± 0.6	2.1 ± 0.6	2.1 ± 0.6	2.1 ± 0.6	2.1 ± 0.6
precipitation	5 ± 9	5 ± 9	5 ± 9	5 ± 9	5 ± 9	5 ± 9
High emissions (IPCC RCP 6.0)						
temperature	2.4 ± 0.7	2.4 ± 0.7	2.5 ± 0.7	2.4 ± 0.7	2.5 ± 0.7	2.4 ± 0.7
precipitation	7 ± 14	7 ± 14	7 ± 14	7 ± 14	7 ± 14	7 ± 13
Highest emissions (IPCC RCP 8.5)						
temperature	3.7 ± 0.8	3.7 ± 0.8	3.7 ± 0.8	3.7 ± 0.8	3.8 ± 0.8	3.7 ± 0.8
precipitation	9 ± 16	9 ± 16	9 ± 16	9 ± 16	9 ± 16	10 ± 16

Table 2. **Climate Change Trends**. Historical rates of change (mean ± standard error) and projected future changes (mean ± standard deviation) in annual average temperature (ºC per century) and total annual precipitation (% per century) (data Daly et al. 2008, IPCC 2013; analysis Wang et al. in preparation). All of the historical temperature trends are statistically significant but none of the precipitation trends are. Temperatures in degrees Fahrenheit (ºF.) are approximately double the number in degrees Celsius (ºC). IPCC = Intergovernmental Panel on Climate Change, SF = San Francisco, NHP = National Historic Park, NHS = National Historic Site, N Mem = National Memorial, RCP = Representative Concentration Pathway.

	Eugene O'Neill NHS	Fort Point NHS	John Muir NHS	Port Chicago N Mem	Rosie the Riveter NHP	SF Maritime NHP
Historical (1895-2010)						
temperature	0.8 ± 0.2	0.9 ± 0.2	0.8 ± 0.2	0.9 ± 0.2	1.2 ± 0.2	0.9 ± 0.3
precipitation	8 ± 9	9 ± 9	12 ± 9	10 ± 10	13 ± 10	12 ± 9
Historical (1950-2010)						
temperature	1.7 ± 0.5	1.6 ± 0.6	1.6 ± 0.6	2.4 ± 0.7	1.3 ± 0.5	1.6 ± 0.7
precipitation	11 ± 26	19 ± 27	17 ± 26	24 ± 26	20 ± 28	22 ± 27
Projected (2000-2100)						
Reduced emissions (IPCC RCP 2.6)						
temperature	1.5 ± 0.6	1.4 ± 0.6	1.4 ± 0.6	1.5 ± 0.6	1.4 ± 0.6	1.4 ± 0.6
precipitation	5 ± 12	5 ± 12	5 ± 12	5 ± 12	5 ± 12	5 ± 12
Low emissions (IPCC RCP 4.5)						
temperature	2.2 ± 0.6	2.1 ± 0.6	2.2 ± 0.6	2.2 ± 0.6	2.2 ± 0.6	2.1 ± 0.6
precipitation	5 ± 9	5 ± 9	5 ± 9	4 ± 9	5 ± 9	5 ± 9
High emissions (IPCC RCP 6.0)						
temperature	2.5 ± 0.7	2.5 ± 0.7	2.5 ± 0.7	2.6 ± 0.7	2.5 ± 0.7	2.5 ± 0.7
precipitation	6 ± 14	7 ± 14	6 ± 14	6 ± 14	7 ± 14	7 ± 14
Highest emissions (IPCC RCP 8.5)						
temperature	3.9 ± 0.9	3.8 ± 0.8	3.9 ± 0.8	4 ± 0.8	3.8 ± 0.8	3.8 ± 0.8
precipitation	8 ± 16	9 ± 16	8 ± 16	8 ± 16	9 ± 16	9 ± 16

Table 3. **Golden Gate National Recreation Area (legislative boundary)**.

Historical average temperatures and temperature trends. SD = standard deviation, SE = standard error, sig. = statistical significance, * $P \leq 0.05$, ** $P \leq 0.01$, *** $P \leq 0.001$.

	1971-2000		1895-2010			1950-2010		
	mean	SD	trend	SE	sig.	trend	SE	sig.
	ºC		ºC century^{-1}			ºC century^{-1}		
Annual	13.8	0.5	0.9	0.2	***	1.4	0.5	*
December-February	10.2	0.8	0.8	0.3	**	1.2	0.5	*
March-May	13	0.9	0.8	0.3	**	2	0.7	*
June-August	16.8	0.5	0.8	0.2	***	1.8	0.6	**
September-November	15.4	0.7	0.9	0.2	***	0.7	0.4	
January	9.7	1	1	0.3	**	2.2	0.7	**
February	11	1.1	0.8	0.3	*	1	0.7	
March	11.9	1.2	0.9	0.4	*	2.7	0.9	**
April	12.8	1.1	0.5	0.3		1.4	0.9	
May	14.2	1.1	1.1	0.3	***	1.9	0.7	*
June	15.9	0.9	0.6	0.3	*	1.8	0.7	*
July	17	0.7	0.6	0.2	**	1.7	0.7	*
August	17.4	0.7	1.2	0.3	***	1.9	0.7	**
September	17.6	1	1.2	0.3	***	0.7	0.8	
October	16.1	0.9	1.1	0.3	***	0.9	0.7	
November	12.6	1.1	0.5	0.3		0.5	0.7	
December	9.8	1.2	0.8	0.3	*	0.5	0.8	

Table 4. **Golden Gate National Recreation Area (legislative boundary)**.

Historical average precipitation totals and precipitation trends. SD = standard deviation, SE = standard error, sig. = statistical significance, * $P \leq 0.05$, ** $P \leq 0.01$, *** $P \leq 0.001$.

	1971-2000		1895-2010			1950-2010		
	mean	SD	trend	SE	sig.	trend	SE	sig.
	mm y^{-1}		% $century^{-1}$			% $century^{-1}$		
Annual	838	303	1	9		7	25	
December-February	469	212	3	13		17	31	
March-May	192	107	-5	16		17	41	
June-August	12	10	2	28		-53	75	
September-November	175	115	3	19		-31	51	
January	177	122	-22	19		-47	45	
February	151	115	5	20		91	52	
March	122	91	-14	22		14	54	
April	49	36	19	22		-25	47	
May	21	28	-19	32		142	88	
June	7	7	-22	35		-43	92	
July	2	4	61	94		-67	254	
August	3	6	75	61		-75	136	
September	10	11	-107	52	*	-122	121	
October	47	40	5	25		-21	71	
November	118	95	13	25		-29	70	
December	133	92	28	22		26	67	

Table 5. **Muir Woods National Monument. Historical average temperatures** and temperature trends of the area within the park boundary. SD = standard deviation, SE = standard error, sig. = statistical significance, * $P \leq 0.05$, ** $P \leq 0.01$, *** $P \leq 0.001$.

	1971-2000		1895-2010			1950-2010		
	mean	SD	trend	SE	sig.	trend	SE	sig.
	ºC		ºC century^{-1}			ºC century^{-1}		
Annual	14	0.5	1	0.2	***	1.3	0.5	*
December-February	9.8	0.8	1	0.3	***	1.1	0.5	*
March-May	13.2	0.9	1.1	0.3	***	1.9	0.8	*
June-August	17.4	0.5	0.8	0.2	***	1.7	0.5	**
September-November	15.6	0.7	1.1	0.2	***	0.6	0.5	
January	9.2	1.1	1.2	0.4	**	2.1	0.7	**
February	10.9	1.1	1	0.4	**	0.8	0.8	
March	11.9	1.2	1.1	0.4	**	2.5	0.9	**
April	13.1	1.2	0.7	0.3	*	1.2	0.9	
May	14.7	1.1	1.3	0.3	***	1.9	0.7	*
June	16.7	0.9	0.7	0.3	*	1.6	0.7	*
July	17.5	0.7	0.6	0.2	*	1.5	0.7	*
August	17.9	0.7	1.3	0.3	***	2	0.7	**
September	17.9	1.1	1.3	0.4	***	0.6	0.8	
October	16.3	0.9	1.2	0.3	***	0.8	0.7	
November	12.5	1.2	0.7	0.3	*	0.4	0.7	
December	9.4	1.3	1	0.4	**	0.3	0.9	

Table 6. **Muir Woods National Monument. Historical average precipitation** totals and precipitation trends of the area within the park boundary. SD = standard deviation, SE = standard error, sig. = statistical significance, * $P \leq 0.05$, ** $P \leq 0.01$, *** $P \leq 0.001$.

	1971-2000		1895-2010			1950-2010		
	mean	SD	trend	SE	sig.	trend	SE	sig.
	mm y^{-1}		% $century^{-1}$			% $century^{-1}$		
Annual	1134	371	-7	9		-2	21	
December-February	598	263	-5	13		4	31	
March-May	271	148	-15	16		7	40	
June-August	16	14	20	27		-47	74	
September-November	258	166	-7	19		-23	50	
January	226	153	-31	19		-70	44	
February	204	146	-8	21		64	49	
March	178	143	-26	23		-1	53	
April	60	40	15	23		-35	47	
May	32	41	-14	30		138	79	
June	9	10	-7	36		-35	103	
July	3	7	69	78		-11	206	
August	5	7	76	48		-92	104	
September	15	18	-111	43	*	-63	114	
October	57	48	6	25		-26	73	
November	185	141	-2	24		-19	65	
December	158	110	34	23		40	74	

Table 7. **Point Reyes National Seashore. Historical average temperatures** and temperature trends of the area within the park boundary. SD = standard deviation, SE = standard error, sig. = statistical significance, * $P \leq 0.05$, ** $P \leq 0.01$, *** $P \leq 0.001$.

	1971-2000		1895-2010			1950-2010		
	mean	SD	trend	SE	sig.	trend	SE	sig.
	ºC		ºC century^{-1}			ºC century^{-1}		
Annual	13.3	0.5	0.9	0.2	***	1.3	0.5	*
December-February	10.1	0.8	0.7	0.3	**	1.1	0.5	*
March-May	12.7	0.9	0.9	0.3	**	1.9	0.8	*
June-August	15.5	0.5	0.9	0.2	***	1.6	0.6	*
September-November	14.8	0.7	1	0.2	***	0.6	0.5	
January	9.6	1.1	0.9	0.3	*	2.1	0.7	*
February	11.1	1.1	0.7	0.3	*	0.8	0.8	
March	11.9	1.2	0.9	0.4	*	2.7	0.9	**
April	12.5	1.1	0.6	0.3		1.4	0.9	
May	13.6	1.1	1.2	0.3	***	1.8	0.7	*
June	15	0.9	0.7	0.3	*	1.7	0.8	*
July	15.6	0.7	0.7	0.2	**	1.4	0.7	
August	16	0.7	1.3	0.3	***	1.7	0.7	*
September	16.5	1.1	1.3	0.3	***	0.7	0.8	
October	15.4	0.9	1.1	0.3	***	0.7	0.8	
November	12.6	1.2	0.5	0.3		0.4	0.7	
December	9.7	1.3	0.6	0.4		0.2	0.9	

Table 8. **Point Reyes National Seashore. Historical average precipitation** totals and precipitation trends of the area within the park boundary. SD = standard deviation, SE = standard error, sig. = statistical significance, * $P \leq 0.05$, ** $P \leq 0.01$, *** $P \leq 0.001$.

	1971-2000		1895-2010			1950-2010		
	mean	SD	trend	SE	sig.	trend	SE	sig.
	mm y^{-1}		% $century^{-1}$			% $century^{-1}$		
Annual	840	306	-3	9		3	25	
December-February	480	218	-2	13		11	31	
March-May	185	103	-6	16		26	41	
June-August	11	12	-1	32		-95	87	
September-November	173	112	0	19		-42	46	
January	180	126	-26	19		-51	45	
February	153	119	-1	21		78	54	
March	115	89	-14	21		22	54	
April	48	34	15	22		-28	48	
May	23	31	-18	33		183	91	*
June	6	8	-22	39		-53	111	
July	2	7	33	128		-132	370	
August	3	7	76	77		-197	167	
September	11	14	-97	50		-151	129	
October	48	38	7	24		-34	67	
November	115	93	7	25		-37	69	
December	137	98	24	21		25	65	

Table 9. **Golden Gate National Recreation Area (legislative boundary).**

Projected temperature increases (ºC), 2000 to 2100, from the average of all general circulation model projections used for IPCC (2013). RCP = representative concentration pathway, SD = standard deviation.

	Emissions Scenarios							
	Reductions RCP2.6		Low RCP4.5		High RCP6.0		Highest RCP8.5	
	mean	SD	mean	SD	mean	SD	mean	SD
Annual	1.4	0.6	2.1	0.6	2.4	0.7	3.7	0.8
December-February	1.4	0.5	2	0.6	2.2	0.7	3.4	0.8
March-May	1.3	0.6	1.8	0.6	2.2	0.6	3.3	0.8
June-August	1.4	0.7	2.2	0.8	2.6	0.8	3.9	0.9
September-November	1.5	0.7	2.4	0.9	2.7	0.8	4.3	1.2
January	1.4	0.5	2	0.6	2.3	0.7	3.5	0.8
February	1.3	0.6	1.9	0.6	2.2	0.6	3.3	0.7
March	1.3	0.7	1.8	0.6	2.1	0.7	3.2	0.9
April	1.3	0.5	1.7	0.6	2.2	0.6	3.2	0.8
May	1.3	0.6	1.9	0.6	2.3	0.7	3.4	0.8
June	1.4	0.8	2.1	0.9	2.4	0.9	3.7	1
July	1.4	0.8	2.2	0.8	2.6	0.9	3.9	1
August	1.5	0.7	2.4	0.7	2.8	0.8	4.2	0.9
September	1.7	0.8	2.6	0.8	2.9	1	4.5	1.1
October	1.5	0.8	2.5	1	2.7	0.9	4.4	1.3
November	1.4	0.6	2.3	1.1	2.5	0.8	4	1.4
December	1.4	0.5	2.1	0.9	2.2	0.8	3.6	1.1

Table 10. **Golden Gate National Recreation Area (legislative boundary).**

Projected precipitation changes (%), 2000 to 2100, from the average of all general circulation model projections used for IPCC (2013). RCP = representative concentration pathway, SD = standard deviation.

	Emissions Scenarios							
	Reductions RCP2.6		Low RCP4.5		High RCP6.0		Highest RCP8.5	
	mean	SD	mean	SD	mean	SD	mean	SD
Annual	5	12	5	9	7	14	9	16
December-February	7	15	11	14	13	19	19	22
March-May	7	16	2	21	2	12	2	26
June-August	24	35	31	63	12	37	40	78
September-November	-2	14	-6	24	-6	20	-12	23
January	9	20	14	20	12	22	23	26
February	7	22	15	24	19	31	27	38
March	7	20	4	20	8	16	9	24
April	8	25	0	25	-6	20	-6	38
May	14	37	2	50	-7	29	-12	48
June	8	35	-7	36	-13	31	-8	44
July	99	220	146	240	142	224	186	311
August	67	112	96	148	51	88	112	146
September	10	63	10	69	4	41	21	82
October	7	32	-8	26	-2	34	-16	32
November	-6	13	-7	28	-9	18	-14	29
December	6	23	4	23	13	25	9	24

Table 11. **Muir Woods National Monument. Projected temperature increases** (ºC), 2000 to 2100, for the area within the park boundary, from the average of all available general circulation model projections used for IPCC (2013). RCP = representative concentration pathway, SD = standard deviation.

	Emissions Scenarios							
	Reductions RCP2.6		Low RCP4.5		High RCP6.0		Highest RCP8.5	
	mean	SD	mean	SD	mean	SD	mean	SD
Annual	1.4	0.6	2.1	0.6	2.5	0.7	3.8	0.8
December-February	1.4	0.5	2	0.6	2.2	0.7	3.4	0.8
March-May	1.3	0.6	1.8	0.6	2.2	0.6	3.3	0.8
June-August	1.4	0.7	2.2	0.8	2.6	0.8	4	0.9
September-November	1.5	0.7	2.4	0.9	2.7	0.8	4.3	1.2
January	1.4	0.6	2	0.6	2.3	0.7	3.5	0.8
February	1.3	0.6	1.9	0.6	2.2	0.6	3.3	0.7
March	1.3	0.7	1.8	0.6	2.2	0.7	3.2	0.9
April	1.3	0.5	1.7	0.6	2.2	0.6	3.2	0.8
May	1.3	0.6	1.9	0.7	2.3	0.7	3.4	0.8
June	1.4	0.8	2.1	0.9	2.5	0.9	3.7	1
July	1.4	0.8	2.2	0.8	2.7	0.9	3.9	1
August	1.5	0.7	2.4	0.7	2.8	0.8	4.2	0.9
September	1.7	0.8	2.6	0.8	2.9	1	4.5	1.1
October	1.5	0.8	2.5	1	2.7	0.9	4.4	1.3
November	1.4	0.6	2.3	1.1	2.5	0.8	4	1.4
December	1.4	0.5	2.1	0.9	2.2	0.7	3.6	1.1

Table 12. **Muir Woods National Monument. Projected precipitation changes** (%), 2000 to 2100, for the area within the park boundary, from the average of all available general circulation model projections used for IPCC (2013). RCP = representative concentration pathway, SD = standard deviation.

	Emissions Scenarios							
	Reductions RCP2.6		Low RCP4.5		High RCP6.0		Highest RCP8.5	
	mean	SD	mean	SD	mean	SD	mean	SD
Annual	5	12	5	9	7	14	9	16
December-February	7	15	10	14	13	19	19	22
March-May	7	16	2	20	2	12	2	26
June-August	23	35	30	62	12	36	38	77
September-November	-2	14	-6	24	-6	19	-12	24
January	9	20	14	20	12	22	23	26
February	7	22	14	24	19	30	27	37
March	7	20	4	20	8	16	8	24
April	8	25	0	25	-6	20	-6	37
May	14	37	2	49	-8	29	-11	48
June	7	35	-7	37	-14	31	-9	44
July	108	252	154	260	157	253	199	342
August	66	114	92	139	51	88	108	144
September	10	61	10	68	4	41	20	82
October	7	32	-8	26	-2	34	-16	32
November	-6	13	-6	28	-9	18	-13	29
December	6	23	4	23	13	25	9	24

Table 13. **Point Reyes National Seashore. Projected temperature increases** (ºC), 2000 to 2100, for the area within the park boundary, from the average of all available general circulation model projections used for IPCC (2013). RCP = representative concentration pathway, SD = standard deviation.

	Emissions Scenarios							
	Reductions RCP2.6		Low RCP4.5		High RCP6.0		Highest RCP8.5	
	mean	SD	mean	SD	mean	SD	mean	SD
Annual	1.4	0.6	2.1	0.6	2.4	0.7	3.7	0.8
December-February	1.3	0.5	2	0.6	2.2	0.7	3.4	0.8
March-May	1.3	0.5	1.8	0.6	2.2	0.6	3.2	0.8
June-August	1.4	0.7	2.2	0.7	2.6	0.8	3.9	0.9
September-November	1.5	0.6	2.4	0.9	2.7	0.8	4.2	1.1
January	1.4	0.5	2	0.6	2.2	0.7	3.4	0.8
February	1.3	0.5	1.9	0.6	2.2	0.6	3.3	0.7
March	1.3	0.7	1.8	0.6	2.1	0.6	3.2	0.8
April	1.3	0.5	1.7	0.6	2.2	0.6	3.1	0.7
May	1.3	0.6	1.9	0.6	2.3	0.7	3.4	0.8
June	1.4	0.8	2	0.8	2.4	0.8	3.7	0.9
July	1.4	0.7	2.2	0.8	2.6	0.8	3.9	0.9
August	1.5	0.7	2.4	0.7	2.8	0.7	4.2	0.9
September	1.7	0.7	2.5	0.8	2.8	0.9	4.4	1.1
October	1.5	0.7	2.4	1	2.7	0.9	4.3	1.2
November	1.4	0.6	2.2	1.1	2.5	0.7	3.9	1.3
December	1.4	0.5	2	0.8	2.2	0.7	3.5	1.1

Table 14. **Point Reyes National Seashore. Projected precipitation changes** (%), 2000 to 2100, for the area within the park boundary, from the average of all available general circulation model projections used for IPCC (2013). RCP = representative concentration pathway, SD = standard deviation.

	Emissions Scenarios							
	Reductions RCP2.6		Low RCP4.5		High RCP6.0		Highest RCP8.5	
	mean	SD	mean	SD	mean	SD	mean	SD
Annual	5	11	5	9	7	13	10	16
December-February	7	15	11	14	13	18	19	21
March-May	8	16	3	20	2	12	2	26
June-August	24	34	29	61	15	41	39	79
September-November	-2	14	-6	24	-6	19	-12	24
January	9	20	14	19	12	21	24	26
February	7	22	15	23	19	29	27	36
March	7	20	5	20	8	16	9	25
April	8	25	0	25	-5	20	-5	37
May	14	38	1	48	-8	29	-11	47
June	8	37	-8	38	-12	32	-9	47
July	106	239	172	273	172	277	218	357
August	65	113	83	119	54	93	103	143
September	7	57	8	64	3	40	19	78
October	6	31	-8	26	-3	33	-16	32
November	-6	14	-6	29	-8	18	-13	29
December	6	23	4	23	13	26	9	24

Table 15. **Ecosystem Carbon**. Aboveground carbon (mean ± 95% confidence interval) and surface area of changes (Gonzalez et al. 2015).

	Golden Gate NRA	Muir Woods NM	Point Reyes NS	Other six parks	
Carbon stock 2010	1100 ± 490	27 ± 28	910 ± 530	3 ± 3	thousand tons
Carbon density 2010	45 ± 19	120 ± 130	39 ± 23	27 ± 20	tons ha^{-1}
Change 2001-2010	+3 ± 1	+0.2 ± 0.2	+19 ± 13	-0.2 ± 0.1	thousand tons
Change 2001-2010	<1	+1 ± 1	+2 ± 1	-5 ± 4	% of amount
Carbon increase	14	9	8	10	% of area
Carbon decrease	6	3	8	2	% of area

References

Ackerly, D.D., W.K. Cornwell, S.B. Weiss, L.E. Flint, and A.L. Flint. 2015. A geographic mosaic of climate change impacts on terrestrial vegetation: Which areas are most at risk? PLoS ONE 10:e0130629. doi:10.1371/journal.pone.0130629.

Anacker, B.L., M. Gogol-Prokurat, K. Leidholm, and S. Schoenig. 2013. Climate change vulnerability assessment of rare plants in California. Madroño 60: 193-210.

Asner, G.P., P.G. Brodrick, C.B. Anderson, N. Vaughn, D.E. Knapp, and R.E. Martin. 2016. Progressive forest canopy water loss during the 2012–2015 California drought. Proceedings of the National Academy of Sciences of the USA 113: E249-E255.

Baer, A., J.K. Wheeler, and J. Pittermann. 2016. Not dead yet: the seasonal water relations of two perennial ferns during California's exceptional drought. New Phytologist 210: 122-132.

Barry, J.P., C.H. Baxter, R.D. Sagarin, and S.E. Gilman. 1995. Climate-related, long-term faunal changes in a California rocky intertidal community. Science 267: 672-675.

Bonfils, C., P.B. Duffy, B.D. Santer, T.M.L. Wigley, D.B. Lobell, T.J. Phillips, and C. Doutriaux. 2008. Identification of external influences on temperatures in California. Climatic Change 87: 43-55.

Bradley, B.A., M. Oppenheimer, and D.S. Wilcove. 2009. Climate change and plant invasions: Restoration opportunities ahead? Global Change Biology 15: 1511-1521.

Bromirski, P.D., R.E. Flick, and D.R. Cayan. 2003. Storminess variability along the California Coast: 1858–2000. Journal of Climate 16: 982-993.

California Department of Fish and Wildlife. 2016. A Rapid Assessment of the Vulnerability of Sensitive Wildlife to Extreme Drought. California Department of Fish and Wildlife, Sacramento, CA.

Callaway, J.C., E.L. Borgnis, R.E. Turner, and C.S. Milan. 2012. Carbon sequestration and sediment accretion in San Francisco Bay tidal wetlands. Estuaries and Coasts 35: 1163-1181.

Carroll, A.L., S.C. Sillett, and R.D. Kramer. 2014. Millennium-scale crossdating and inter-annual climate sensitivities of standing California redwoods. PLoS One 9: e102545. doi:10.1371/journal.pone.0102545.

Cheung, W.W.L., R.D. Brodeur, T.A. Okey, and D. Pauly. 2015. Projecting future changes in distributions of pelagic fish species of Northeast Pacific shelf seas. Progress in Oceanography 130: 19-31.

Church, J.A. and N.J. White. 2011. Sea-level rise from the late 19th to the early 21st Century.

Surveys in Geophysics 32: 585-602.

Cloern, J.E., N. Knowles, L.R. Brown, D. Cayan, M.D. Dettinger, T.L. Morgan, D.H. Schoellhamer, M.T. Stacey, M. van der Wegen, R.W. Wagner, and A.D. Jassby. 2011. Projected evolution of California's San Francisco Bay-delta-river system in a century of climate change. PLoS ONE 6: e24465. doi:10.1371/journal.pone.0024465.

CMG Landscape Architecture. 2016. Crissy Field + Sea Level Rise-Up. CMG, San Francisco, CA.

Daly, C., M. Halbleib, J.I. Smith, W.P. Gibson, M.K. Doggett, G.H. Taylor, J. Curtis, and P.P. Pasteris. 2008. Physiographically sensitive mapping of climatological temperature and precipitation across the conterminous United States. International Journal of Climatology 28: 2031-2064.

Diffenbaugh, N.S., D.L. Swain, and D. Touma. 2015. Anthropogenic warming has increased drought risk in California. Proceedings of the National Academy of Sciences of the USA 112: 3931-3936.

Dugger, K.M., E.D. Forsman, A.B. Franklin, R.J. Davis, G.C. White, C.J. Schwarz, K.P. Burnham, J.D. Nichols, J.E. Hines, C.B. Yackulic, P.F. Doherty, L. Bailey, D.A. Clark, S.H. Ackers, L.S. Andrews, B. Augustine, B.L. Biswell, J. Blakesley, P.C. Carlson, M.J. Clement, L.V. Diller, E.M. Glenn, A. Green, S.A. Gremel, D.R. Herter, J.M. Higley, J. Hobson, R.B. Horn, K.P. Huyvaert, C. McCafferty, T. McDonald, K. McDonnell, G.S. Olson, J.A. Reid, J. Rockweit, V. Ruiz, J. Saenz, and S.G. Sovern. 2016. The effects of habitat, climate, and Barred Owls on long-term demography of Northern Spotted Owls The Condor 118: 57-116.

Fernández, M., H.H. Hamilton, and L.M. Kueppers. 2015. Back to the future: Using historical climate variation to project near-term shifts in habitat suitable for coast redwood. Global Change Biology 21: 4141-4152.

Franklin, A.B., D.R. Anderson, R.J. Gutiérrez, and K.P. Burnham. 2000. Climate, habitat quality, and fitness in northern spotted owl populations in northwestern California. Ecological Monographs 70: 539-590.

Funayama, K., E. Hines, J. Davis, and S. Allen. 2013. Effects of sea-level rise on northern elephant seal breeding habitat at Point Reyes Peninsula, California. Aquatic Conservation: Marine and Freshwater Ecosystems 23: 233-245.

García-Reyes, M. and J. Largier. 2010. Observations of increased wind-driven coastal upwelling off central California. Journal of Geophysical Research 115: C04011.

doi:10.1029/2009JC005576.

Gardali, T., N.E. Seavy, R.T. DiGaudio, and L.A. Comrack. 2012. A climate change vulnerability assessment of California's at-risk birds. PLoS One 7: e29507. doi:10.1371/journal.pone.0029507.

Glenn, E.M., R.G. Anthony, E.D. Forsman, and G.S. Olson. 2011. Local weather, regional climate, and annual survival of the northern spotted owl. The Condor 113: 159-176.

Gonzalez, P., J.J. Battles, B.M. Collins, T. Robards, and D.S. Saah. 2015. Aboveground live carbon stock changes of California wildland ecosystems, 2001-2010. Forest Ecology and Management 348: 68-77.

Gruber, N., C. Hauri, Z. Lachkar, D. Loher, T.L. Frölicher, and G.K. Plattner. 2012. Rapid progression of ocean acidification in the California Current System. Science 337: 220-223.

Hameed, S.O., K.A. Holzer, A.N. Doerr, J.H. Baty, and M.W. Schwartz. 2013. The value of a multi-faceted climate change vulnerability assessment to managing protected lands: Lessons from a case study in Point Reyes National Seashore. Journal of Environmental Management 121: 37-47.

Hoover, D.J., K.O. Odigie, P.W. Swarzenski, and P. Barnard. in press. Sea-level rise and coastal groundwater inundation and shoaling at select sites in California, USA. Journal of Hydrology: Regional Studies. doi:10.1016/j.ejrh.2015.12.055.

Hutto, S.V., K.D. Higgason, J.M. Kershner, W.A. Reynier, and D.S. Gregg. 2015. Climate Change Vulnerability Assessment for the North-central California Coast and Ocean. Marine Sanctuaries Conservation Series ONMS-15-02. National Oceanic and Atmospheric Administration, Silver Spring, Maryland.

Intergovernmental Panel on Climate Change (IPCC). 2000. Emissions Scenarios. Cambridge University Press, Cambridge, UK.

Intergovernmental Panel on Climate Change (IPCC). 2007. Climate Change 2007: The Physical Science Basis. Cambridge University Press, Cambridge, UK.

Intergovernmental Panel on Climate Change (IPCC). 2013. Climate Change 2013: The Physical Science Basis. Cambridge University Press, Cambridge, UK.

Intergovernmental Panel on Climate Change (IPCC). 2014. Climate Change 2014: Impacts, Adaptation, and Vulnerability. Cambridge University Press, Cambridge, UK.

Johnstone, J.A. and T.E. Dawson. 2010. Climatic context and ecological implications of summer fog decline in the coast redwood region. Proceedings of the National Academy of Sciences of the USA 107: 4533-4538.

Katz, J., P.B. Moyle, R.M. Quiñones, J. Israel, and S. Purdy. 2013. Impending extinction of salmon, steelhead, and trout (*Salmonidae*) in California. Environmental Biology of Fishes 96: 1169-1186.

Keiper, C.A., D.G. Ainley, S.G. Allen, and J.T. Harvey. 2005. Marine mammal occurrence and ocean climate off central California, 1986 to 1994 and 1997 to 1999. Marine Ecology Progress Series 289: 285-306.

Knowles, N. and D. Cayan. 2004. Elevational dependence of projected hydrologic changes in the San Francisco Estuary and watershed. Climatic Change 62: 319-336.

Knowles, N. and D.R. Cayan. 2002. Potential effects of global warming on the Sacramento/San Joaquin watershed and the San Francisco estuary. Geophysical Research Letters 29: 1891. doi:10.1029/2001GL014339.

La Sorte, F.A. and F.R. Thompson. 2007. Poleward shifts in winter ranges of North American birds. Ecology 88: 1803-1812.

Largier, J.L, B.S. Cheng, and K.D. Higgason (Eds.) 2011. Climate Change Impacts: Gulf of the Farallones and Cordell Bank National Marine Sanctuaries. Office of National Marine Sanctuaries Report ONMS-11-04, National Oceanic and Atmospheric Administration, Silver Spring, MD.

Lewitus, A.J., R.A. Horner, D.A. Caron, E. Garcia-Mendoza, B.M. Hickey, M. Hunter, D.D. Huppert, R.M. Kudela, G.W. Langlois, J.L. Largier, E.J. Lessard, R. RaLonde, J.E.J. Rensel, P.G. Strutton, V.L. Trainer, J.F. Tweddle. 2012. Harmful algal blooms along the North American west coast region: History, trends, causes, and impacts. Harmful Algae 19: 133-159.

Littell, J.S., D. McKenzie, D.L. Peterson, and A.L. Westerling. 2009. Climate and wildfire area burned in western U.S. ecoprovinces, 1916–2003. Ecological Applications 19: 1003-1021.

Marlon, J.R., P.J. Bartlein, D.G. Gavin, C.J. Long, R.S. Anderson, C.E. Briles, K.J. Brown, D. Colombaroli, D.J. Hallett, M.J. Power, E.A. Scharf, and M.K. Walsh. 2012. Long-term perspective on wildfires in the western USA. Proceedings of the National Academy of Sciences of the USA 109: E535-E543.

Metz, M.R., J.M. Varner, K.M. Frangioso, R.K. Meentemeyer, and D.M. Rizzo. 2013. Unexpected redwood mortality from synergies between wildfire and an emerging infectious disease. Ecology 94: 2152-2159.

Moore, S.E. and H.P. Huntington. 2008. Arctic marine mammals and climate change: Impacts and resilience. Ecological Applications 18: S157-S165.

Moore, S.K., V.L. Trainer, N.J. Mantua, M.S. Parker, E.A. Laws, L.C. Backer, and L.E. Fleming. 2008. Impacts of climate variability and future climate change on harmful algal blooms and human health. Environmental Health 7: S4. doi: 10.1186/1476-069X-7-S2-S4.

Moss, R.H., J.A. Edmonds, K.A. Hibbard, M.R. Manning, S.K. Rose, D.P. van Vuuren, T.R. Carter, S. Emori, M. Kainuma, T. Kram, G.A. Meehl, J.F.B. Mitchell, N. Nakicenovic, K. Riahi, S.J. Smith, R.J. Stouffer, A.M. Thomson, J.P. Weyant, and T.J. Wilbanks. 2010. The next generation of scenarios for climate change research and assessment. Nature 463: 747-756.

National Research Council. 2012. Sea-Level Rise for the Coasts of California, Oregon, and Washington: Past, Present, and Future. National Academies Press, Washington, DC.

Newland, M. 2013. The Potential Effects of Climate Change on Cultural Resources within Point Reyes National Seashore, Marin County, California. Sonoma State University, Rohnert Park, CA.

O'Neil, J.M., T.W. Davis, M.A. Burford, and C.J. Gobler. 2012. The rise of harmful cyanobacteria blooms: The potential roles of eutrophication and climate change. Harmful Algae 14: 313-334.

Paprocki, N. 2014. Regional distribution shifts help explain local changes in wintering raptor abundance: Implications for interpreting population trends. PLOS One 9: e86814-e86814.

Peek, K.M., R.S. Young, R.L. Beavers, C.H. Hoffman, B.T. Diethorn, and S. Norton. 2015. Adapting to climate change in coastal national parks: Estimating the exposure of park assets to 1 m of sea-level rise. Natural Resource Report NPS/NRSS/GRD/NRR—2015/961. National Park Service, Fort Collins, CO.

Pendleton, E.A., E.R. Thieler, and S.J. Williams. 2010. Importance of coastal change variables in determining vulnerability to sea- and lake-level change. Journal of Coastal Research 26: 176-183.

Pendleton, L., D.C. Donato, B.C. Murray, S. Crooks, W.A. Jenkins, S. Sifleet, C. Craft, J.W. Fourqurean, J.B. Kauffman, N. Marbà, P. Megonigal, E. Pidgeon, D. Herr, D. Gordon, and A. Baldera. 2012. Estimating global "blue carbon" emissions from conversion and degradation of vegetated coastal ecosystems. PLoS ONE 7: e43542. doi:10.1371/journal.pone.0043542.

Rapacciuolo, G., S.P. Maher, A.C. Schneider, T.T. Hammond, M.D. Jabis, R.E. Walsh, K.J. Iknayan, G.K. Walden, M.F. Oldfather, D.D. Ackerly, and S.R. Beissinger. 2014. Beyond a warming fingerprint: Individualistic biogeographic responses to heterogeneous climate

change in California. Global Change Biology 20: 2841-2855.

Sagarin, R.D., J.P. Barry, S.E. Gilman, and C.H. Baxter. 1999. Climate-related change in an intertidal community over short and long time scales. Ecological Monographs 69: 465-490.

Sandel, B. and E.M. Dangremond. 2012. Climate change and the invasion of California by grasses. Glob Change Biology 18: 277-289.

Scholin, C.A., F. Gulland, G.J. Doucette, S. Benson, M. Busman, F.P. Chavez, J. Cordaro, R. DeLong, A. De Vogelaere, J. Harvey, M. Haulena, K. Lefebvre, T. Lipscomb, S. Loscutoff, L.J. Lowenstine, R. Marin, P.E. Miller, W.A. McLellan, P.D.R. Moeller, C.L. Powell, T. Rowles, P. Silvagni, M. Silver, T. Spraker, V. Trainer, and F.M. Van Dolah. 2000. Mortality of sea lions along the central California coast linked to a toxic diatom bloom. Nature 403: 80-84.

Sillett, S.C., R. Van Pelt, G.W. Koch, A.R. Ambrose, A.L. Carroll, M.E. Antoine, and B.M. Mifsud. 2010. Increasing wood production through old age in tall trees Forest Ecology and Management 259: 976-994.

Spies, B.T. and M.A. Steele. 2016. Effects of temperature and latitude on larval traits of two estuarine fishes in differing estuary types. Marine Ecology Progress Series 544: 243–255.

Sydeman, W.J. and S.G. Allen. 1999. Pinniped population dynamics in central California: Correlations with sea surface temperature and upwelling indices. Marine Mammal Science 15: 446-461.

Sydeman, W.J., M. García-Reyes, D.S. Schoeman, R.R. Rykaczewski, S.A. Thompson, B.A. Black, and S.J. Bograd. 2014. Climate change and wind intensification in coastal upwelling ecosystems. Science 345: 77-80.

Sydeman, W.J., M.M. Hester, J.A Thayer, F. Gress, P. Martin, and J. Buffa. 2001. Climate change, reproductive performance and diet composition of marine birds in the southern California Current system, 1969–1997. Progress in Oceanography 49: 309-329.

Thorne, J.H., R.M. Boynton, L.E. Flint, and A.L. Flint. 2015. The magnitude and spatial patterns of historical and future hydrologic change in California's watersheds. Ecosphere 6:24. doi:10.1890/ES14-00300.1.

Thorne, J.H., R.M. Boynton, A.J. Holguin, J.A.E. Stewart, and J. Bjorkman. 2016. A climate change vulnerability assessment of California's terrestrial vegetation. California Department of Fish and Wildlife, Sacramento, CA.

Trouet, V., A.H. Taylor, E.R. Wahl, C.N. Skinner, and S.L. Stephens. 2010. Fire-climate interactions in the American West since 1400 CE. Geophysical Research Letters 37:

L04702. doi:10.1029/2009GL041695.

Van Pelt, R., S.C. Sillett, W.A. Kruse, J.A. Freund, NS R.D. Kramer. 2016. Emergent crowns and light-use complementarity lead to global maximum biomass and leaf area in Sequoia sempervirens forests. Forest Ecology and Management 375: 279-308.

Walsh, J., D. Wuebbles, K. Hayhoe, J. Kossin, K. Kunkel, G. Stephens, P. Thorne, R. Vose, M. Wehner, and J. Willis. 2014. Our changing climate. In Melillo, J.M., T.C. Richmond, and G. W. Yohe (Eds.) Climate Change Impacts in the United States: The Third National Climate Assessment. U.S. Global Change Research Program, Washington, DC.

Wang, D., T.C. Gouhier, B.A. Menge, and A.R. Ganguly. 2015. Intensification and spatial homogenization of coastal upwelling under climate change. Nature 518: 390-394.

Wang, F., P. Gonzalez, M. Notaro, D. Vimont, and J.W. Williams. in preparation. Significant historical and projected climate change in U.S. national parks.

Wells, R.S., L.J. Hansen, A.B. Baldridge, T.P. Dohl, D.L. Kelly, and R.H. Defran. 1990. Northward extension of the ranges of bottlenose dolphins along the California coast. In Leatherwood, S. and R.R. Reeves (eds) The Bottlenose Dolphin. Academic Press, San Diego, CA.

Westerling, A.L., B.P. Bryant, H.K. Preisler, T.P. Holmes, H.G. Hidalgo, T. Das, and S.R. Shrestha. 2011. Climate change and growth scenarios for California wildfire. Climatic Change 109: S445-463.

Williams, A.P., R. Seager, J.T. Abatzoglou, B.I. Cook, J.E. Smerdon, and E.R. Cook. 2015. Contribution of anthropogenic warming to California drought during 2012–2014. Geophysical Research Letters 42: 6819-6828.

Wolf, A., N.B. Zimmerman, W.R.L. Anderegg, P.E. Busby, and J. Christensen. 2016. Altitudinal shifts of the native and introduced flora of California in the context of 20th-century warming. Global Ecology and Biogeography 25: 418-429.

Wood, A.W., L.R. Leung, V. Sridhar and D.P. Lettenmaier. 2004. Hydrologic implications of dynamical and statistical approaches to downscaling climate model outputs. Climatic Change 62: 189-216.